Towards a generalized hydrodynamics description of Rényi entropies in integrable systems

Vincenzo Alba
International School for Advanced Studies (SISSA), Via Bonomea 265, 34136, Trieste, Italy, INFN, Sezione di Trieste

(Received 22 August 2018; published 29 January 2019)

We investigate the steady-state Rényi entanglement entropies after a quench from a piecewise homogeneous initial state in integrable models. In the quench protocol, two macroscopically different chains (leads) are joined together at the initial time, and the subsequent dynamics is studied. We study the entropies of a finite subsystem at the interface between the two leads. The density of Rényi entropies coincides with that of the entropies of the generalized Gibbs ensemble that describes the interface between the chains. By combining the generalized hydrodynamics treatment of the quench with the Bethe ansatz approach for the Rényi entropies, we provide exact results for quenches from several initial states in the anisotropic Heisenberg chain (XXZ chain), although the approach is applicable, in principle, to any low-entangled initial state and any integrable model. An interesting protocol that we consider is the *expansion quench*, in which one of the two leads is prepared in the vacuum of the model excitations. An intriguing feature is that for moderately large anisotropy the transport of bound state is not allowed. Moreover, we show that there is a "critical" anisotropy, below which bound-state transport is permitted. This is reflected in the steady-state entropies, which for large enough anisotropy do not contain information about the bound states. Finally, we benchmark our results against time-dependent density matrix renormalization group simulations.

DOI: 10.1103/PhysRevB.99.045150

I. INTRODUCTION

In recent years, entanglement-related quantities emerged as informative witnesses of the complexity of the quantum many-body wave function, both at equilibrium and out of equilibrium. Entanglement is deeply intertwined with the computational cost to accurately describe the quantum many-body wave function by using matrix product states [1–4]. The Rényi entropies $S^{(\alpha)}$ are popular entanglement measures for pure states. Given a subsystem A', they are defined as

$$S^{(\alpha)} \equiv \frac{1}{1-\alpha} \ln \mathrm{Tr} \rho_{A'}^{\alpha}, \quad \text{with } \alpha \in \mathbb{R} \tag{1}$$

where $\rho_{A'}$ is the reduced density matrix of A'. The limit $\alpha \to 1$ in (1) defines the von Neumann entropy as $S \equiv -\mathrm{Tr}\rho_{A'} \ln \rho_{A'}$. The knowledge of Rényi entropies for different values of α gives access to the distribution of the full spectrum of $\rho_{A'}$ [5] (entanglement spectrum). Importantly, the Rényi entropies can be computed by using quantum and classical Monte Carlo methods [6], and can be measured in experiments with cold atoms [7–10], unlike the von Neumann entropy.

Rényi and von Neumann entropies are key to understanding the fundamental physics underlying thermalization in isolated out-of-equilibrium systems, for instance, after a quantum quench. This is the standard protocol to drive a system out of equilibrium: A system is prepared initially in a low-entanglement state $|\Psi_0\rangle$, and it is let to evolve with a local Hamiltonian H, such that $[H, |\Psi_0\rangle\langle\Psi_0|] \neq 0$. It is by now accepted that for generic systems local properties of the steady-state emerging at late times can be described by the Gibbs (thermal) ensemble, whereas for integrable models one has to use a generalized Gibbs ensemble (GGE) [11–39]. Quite generically, the Rényi entropies (and the von Neumann entropy) exhibit a linear growth at short times, which is followed by a saturation at late times. Their short-time behavior reflects the irreversible growth of the complexity of the system after the quench, whereas their steady-state value coincides with generalized (GGE) free energies [40–42]. These qualitative features, i.e., the linear growth and the saturation behavior, appear to be ubiquitous [4,43–70].

A well-known quasiparticle picture allows to understand the qualitative behavior of the entanglement spreading [43]. In this picture, the entanglement growth is the result of the ballistic propagation of entangled pairs of quasiparticles created after the quench. For noninteracting fermion models, the quasiparticle picture is exact in the scaling limit, as it has been demonstrated in Ref. [44]. Remarkably, for integrable interacting models, by complementing the semiclassical picture with thermodynamic knowledge of the steady state, it is possible to describe quantitatively the full-time dynamics of the von Neuamann entropy [45,71]. Unfortunately, a generalization of this result to the Rényi entropies is not available yet, although the thermodynamic Bethe ansatz (TBA) can be used (see Refs. [40–42]) to obtain the steady-state Rényi entropies.

Recent years witnessed an enormous interest in quenches from piecewise homogeneous initial conditions. Several techniques have been used, such as conformal field theory [72–77] (CFT), free-fermion methods [78–89], field theory methods [90–92], integrability [93–97], and numerical techniques [89,98–102]. For integrable models, the recently developed generalized hydrodynamics (GHD) [103,104] allows for an analytic treatment of these quenches [105–122]. The standard setup that we consider is depicted in Fig. 1. This is the prototypical situation to study quantum transport in one-dimensional system. Two chains A and B are prepared

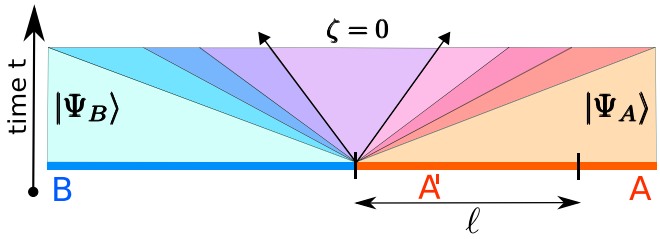

FIG. 1. Rényi entropies after a quench from a piecewise homogeneous initial condition in integrable systems: setup considered in this work. Two chains A and B are prepared in the states $|\Psi_A\rangle$ and $|\Psi_B\rangle$ and are joined together at $t = 0$. In the space-time scaling limit on each ray ζ dynamical properties are described by a generalized Gibbs ensemble (GGE). Here, we focus on the Rényi entropies of a subregion A' of length ℓ placed next to the interface between A and B.

in two macroscopically different states. At $t = 0$ they are connected, and the full system is let to evolve unitarily under a many-body Hamiltonian H. In the GHD approach, in the scaling limit of long time t and large distance x, at fixed $\zeta \equiv x/t$ (rays in Fig. 1) dynamical properties are described by a GGE. However, as of now, only few results have been derived for the entanglement dynamics after quenches from piecewise homogeneous states. Notable exceptions are systems that can be mapped to CFTs in curved space-time [75–77]. Also, for free-fermion systems, the full-time dynamics of the entanglement entropies has been derived analytically in Ref. [68]. For interacting integrable models a conjecture for the steady-state von Neumann entropy and for the entanglement production rate at short times has been presented in Ref. [64].

However, extending the quasiparticle picture to describe the Rényi entropies after quenches from piecewise homogeneous states remains an open problem. The aim of this work is to provide a step forward in this direction. Here, we focus on the steady-state Rényi entropies of a finite subregion A' of length ℓ placed next to the interface between A and B (see Fig. 1). The key idea is that in the limit $\ell/t \to 0$, the entire subsystem A' should be described by the GGE with $\zeta = 0$, i.e., by the NESS (nonequilibrium steady state). Thus, following Ref. [40], the density of Rényi entropy has to coincide with that of the NESS Rényi entropy, which can be calculated using the thermodynamic Bethe ansatz (TBA). Specifically, the appropriate thermodynamic ensemble that determines the Rényi entropies is obtained by combining the GHD approach for the quench [103,104] with the results of Ref. [40]. By using this method, we investigate the Rényi entropy after quenches in the spin-$\frac{1}{2}$ anisotropic Heisenberg chain (XXZ chain). We consider several initial states for A and B, such as the Néel state and the Majumdar-Ghosh state. However, in principle, our approach is straightforwardly generalizable to any low-entangled initial state (product state) and to any integrable model. For all these quenches, we provide robust numerical evidence for our results by using the time-dependent density matrix renormalization group (tDMRG) method [123–126].

Finally, we consider the quench in which A is initially prepared in the ferromagnetic state. After mapping the Heisenberg chain onto a system of interacting fermions confined in a box, this corresponds to the trap-expansion protocol that is routinely performed in cold-atom experiments. For this reason, we term this quench *expansion quench*.

A remarkable feature of the XXZ chain is that its spectrum contains composite excitations, which consist of bound states of several elementary particles (magnons). The physics of these bound states is receiving constant attention, both theoretically [127–132], as well as experimentally [133,134]. Interestingly, while for generic quenches, the steady-state entropies contain information about all the types of quasiparticles (bound and unbound states), this is not the case for the expansion quench, at least in the limit of large anisotropy. Here, we show that this reflects that the bound-state transport between the two chains is not possible at large anisotropy. This is an intriguing effect of the interactions, which renormalize the group velocity of the "bare" excitations of the model. Physically, after the expansion quench, the velocities of the bound states created in the bulk of A and B change their sign when approaching the interface, and they are deflected back. This suggests that the expansion quench could be used as a filter to isolate multispin bound states. An interesting result is that there is a "critical" anisotropy, below which dynamical properties change abruptly, and the bound-state transport is permitted. We explicitly check this scenario for the expansion of the Néel state and the Majumdar-Ghosh state, although we expect it to happen for a larger class of initial states.

The paper is organized as follows. In Secs. II A and II B we review the thermodynamic Bethe ansatz (TBA) approach for homogeneous quantum quenches in integrable models, focusing on the steady-state Rényi entropies in Sec. II C. In Sec. III A we review the generalized hydrodynamic approach (GHD). In Sec. III B we discuss the steady-state Rényi entropies. In Sec. IV A we present the XXZ chain and the quench protocols. In Secs. IV B and IV C we discuss the expansion quench and its GHD solution, highlighting the absence of bound-state transport for large anisotropy. In Sec. IV D we report some exact results for the expansion quenches of the Néel and the Majumdar-Ghosh state in the limit of large anisotropy. In Sec. IV E we present theoretical predictions for the steady-state Rényi entropies after the expansion quench. Numerical results are presented in Sec. IV F. Finally, these are benchmarked against tDMRG simulations in Sec. V.

II. RÉNYI ENTROPIES AFTER A HOMOGENEOUS QUENCH

Here, we summarize the TBA approach introduced in Ref. [40] (see also Refs. [41,42]) to calculate the steady-state Rényi entropies after a homogeneous quench. First, in Sec. II A we review some general aspects of the TBA approach for integrable models. In Sec. II B we discuss the TBA treatment for quenches. Section II C is devoted to discussing how to calculate the entropies using TBA.

A. Thermodynamic Bethe ansatz (TBA) for integrable models

The distinctive feature of integrable models is that they possess families of well-defined and stable, i.e., having infinite lifetime, quasiparticles. Different quasiparticles are labeled

by their quasimomentum (rapidity) that we denote as λ. A generic eigenstate of a Bethe ansatz solvable model is in a one-to-one correspondence with a set of allowed quasiparticle rapidities, which are obtained by solving a system of nonlinear algebraic equations known as Bethe equations [135]. In the thermodynamic limit, the rapidities form a continuum, and it is more convenient to work with the rapidity density $\boldsymbol{\rho}$ (particle densities) and the hole densities $\boldsymbol{\rho}^{(h)}$, i.e., the density of unoccupied rapidities. Here, we defined $\boldsymbol{\rho} \equiv \{\rho_n\}_{n=1}^{\mathcal{N}}$ and $\boldsymbol{\rho}^{(h)} \equiv \{\rho_n^{(h)}\}_{n=1}^{\infty}$, where n labels the different quasiparticle families. Their total number $\mathcal{N}$ depends on the model under consideration. For instance, in the XXZ chain with $\Delta \geqslant 1$, which is the model considered here, there are infinite families of quasiparticles, i.e., $\mathcal{N} = \infty$. For the XXZ chain, the quasiparticles with $n = 1$ correspond to free-magnon-like excitations, whereas the ones with $n > 1$ are bound states of n down spins. For later convenience, we also define the total densities $\rho_n^{(t)}$, the densities η_n, and the filling functions ϑ_n as

$$\rho_n^{(t)} \equiv \rho_n + \rho_n^{(h)}, \tag{2}$$

$$\eta_n \equiv \rho_n^{(h)} \rho_n^{-1}, \tag{3}$$

$$\vartheta_n \equiv [1 + \eta_n]^{-1}. \tag{4}$$

In any Bethe ansatz solvable model, the particle densities ρ_n are coupled to the η_n via the thermodynamic version of the Bethe equations, which read as [135]

$$2\pi \rho_n (1 + \eta_n) = a_n - \sum_{m=1}^{\infty} a_{nm} \star \rho_m. \tag{5}$$

Here, the functions $a_n(\lambda)$ and $a_{nm}(\lambda)$ are known from the Bethe ansatz solution of the model. For the XXZ chain a_n and a_{nm} are given as [135]

$$a_n = \frac{1}{\pi} \frac{\sinh(n\eta)}{\cosh(n\eta) - \cos(2\lambda)}, \tag{6}$$

$$a_{nm} = (1 - \delta_{nm}) a_{|n-m|} + a_{|n-m|+2} + \cdots + a_{n+m-2} + a_{n+m}. \tag{7}$$

Here, $\eta \equiv \operatorname{arccosh}(\Delta)$. The matrix a_{nm} encodes the scattering between quasiparticles of different families, and with different rapidities. In (5) the symbol $\star$ denotes the convolution

$$f \star g \equiv \int d\mu \, f(\lambda - \mu) g(\mu). \tag{8}$$

Any set of densities $\boldsymbol{\rho}$ identifies a thermodynamic macrostate, which corresponds to an exponentially diverging (with size) number of microscopic eigenstates. Any of these eigenstates can be chosen as a finite-size representative of the thermodynamic macrostate. The total number of equivalent microstates is given as $e^{S_{\rm YY}}$, with $S_{\rm YY}$ the so-called Yang-Yang entropy [135]

$$S_{\rm YY}(\boldsymbol{\rho}) \equiv L \sum_n \int d\lambda \big\{ \rho_n^{(t)} \ln \rho_n^{(t)} - \rho_n^{(h)} \ln \rho_n^{(h)} - \rho_n \ln \rho_n \big\}, \tag{9}$$

where L is the system size. The Yang-Yang entropy is extensive and it is obtained by summing independently over the quasiparticle families and their rapidity, reflecting, again, the integrability. For systems in thermal equilibrium $S_{\rm YY}$ is the thermal entropy. For out-of-equilibrium systems, the density of the Yang-Yang entropy of the GGE that describes the steady state is a key ingredient to understand quantitatively the dynamics of the entanglement entropy after the quench [45,71].

B. TBA description of homogeneous quenches

Integrable models solvable by the Bethe ansatz possess an extensive number of local and quasilocal conserved quantities $\hat{Q}_k$, i.e., having the property that $[\hat{Q}_j, \hat{Q}_k] = 0, \ \forall \ j, k$, with $\hat{Q}_2$ being the Hamiltonian. This implies that, due to these conservation laws, in integrable models the out-of-equilibrium dynamics after a quantum quench, and the steady state, are strongly constrained. As a consequence, at late times the system fails to thermalize, i.e., *local* properties are not described by the Gibbs ensemble. Still, it is now accepted that local and quasilocal properties of the steady state are described by a generalized Gibbs ensemble (GGE). The GGE density matrix is obtained by complementing the Gibbs density matrix with the extra conserved quantities $\hat{Q}_j$, to obtain

$$\rho_{\rm GGE} = \frac{1}{Z_{\rm GGE}} \exp\Big(- \sum_k \beta_k \hat{Q}_k \Big). \tag{10}$$

Here, β_k is the Lagrange multiplier associated with $\hat{Q}_k$ and $Z_{\rm GGE}$ is a normalization constant (GGE partition function). The β_k are fixed by imposing that the GGE average of $\hat{Q}_k$ equals their initial state value as

$$\operatorname{Tr}(\rho_{\rm GGE} \hat{Q}_k) = \langle \Psi_0 | \hat{Q}_k | \Psi_0 \rangle. \tag{11}$$

The key idea of the TBA approach for quantum quenches is that GGE expectation values of local and quasilocal observables are described by a carefully chosen thermodynamic macrostate (see Sec. II A), which can be completely characterized in terms of the initial state expectation values of the conserved quantities [136] [cf. (11)].

We now illustrate how to determine this macrostate by using the TBA. First, in the thermodynamic limit, the expectation value $\hat{Q}_k$ over a generic thermodynamic macrostate identified by particle and hole distributions ρ_n, $\rho_n^{(h)}$ is obtained by summing over the quasiparticle families and integrating over their rapidities as [135]

$$Q_k = L \sum_n \int d\lambda \, f_{kn}(\lambda) \rho_n(\lambda), \tag{12}$$

where we introduced the functions f_{kn}, and L is the system size. It is convenient to define the generalized driving g_n as

$$g_n(\lambda) \equiv \sum_k \beta_k f_{kn}. \tag{13}$$

The driving g_n contains the crucial information about the initial values of the conserved charges or, equivalently, on β_k.

To proceed, it is useful to consider the GGE expectation value $\operatorname{Tr}\rho_{\rm GGE}\hat{\mathcal{O}}$ of a generic local (or quasilocal) observable $\hat{\mathcal{O}}$. In the thermodynamic limit, the trace over the model eigenstates becomes a functional integral as

$$\operatorname{Tr} \to \int D\rho \, e^{S_{\rm YY}(\rho)}. \tag{14}$$

Here, $D\rho \equiv \prod_n D\rho_n$ denotes the functional integral over the densities ρ_n. The Yang-Yang entropy in (14) takes into account that a thermodynamic macrostate corresponds to an exponentially large number of eigenstates. Using (14), one can write

$$\mathrm{Tr}(\hat{\mathcal{O}}\rho_{\mathrm{GGE}}) = \frac{1}{Z_{\mathrm{GGE}}} \int D\rho\, e^{-\mathcal{E}(\rho)+S_{\mathrm{YY}}(\rho)} \langle\rho|\hat{\mathcal{O}}|\rho\rangle. \tag{15}$$

Here, we defined $\mathcal{E}(\rho)$ as

$$\mathcal{E} = L \sum_n \int d\lambda\, g_n(\lambda)\rho_n(\lambda). \tag{16}$$

In (15), $\langle\rho|\hat{\mathcal{O}}|\rho\rangle$ denotes the value of $\hat{\mathcal{O}}$ over the macrostate. Importantly, the locality and quasilocality of $\hat{Q}_k$ implies that $\mathcal{E}$ is extensive, as it is clear from (16). Due to the extensivity of $\mathcal{E}$ and S_{YY}, following the standard TBA approach [135], in the thermodynamic limit the integral in (15) can be treated using the saddle-point method. One has to minimize the functional $\mathcal{S}_{\mathrm{GGE}}$ defined as

$$\mathcal{S}_{\mathrm{GGE}} \equiv -\mathcal{E} + S_{\mathrm{YY}}. \tag{17}$$

After minimizing (17) with respect to ρ_n, one obtains a set of generalized TBA equations for η_n [see (4)] as

$$\ln \eta_n = g_n + \sum_{m=1}^{\infty} a_{nm} \star \ln\left[1+\eta_m^{-1}(\lambda)\right], \tag{18}$$

where a_{nm} is the same as in (5), and g_n is defined in (13). Finally, the GGE macrostate densities ρ_n are obtained by substituting the solutions of (18) in the TBA equations (5).

C. TBA approach for Rényi entropies

Here, we discuss how to calculate the steady-state value of the Rényi entanglement entropies after a homogeneous quench in integrable systems [40,41]. Since local properties of the steady state are described by a GGE, the density of Rényi entanglement entropies has to coincide with that of the GGE Rényi entropies $S^{(\alpha)}_{\mathrm{GGE}}$. These are defined as

$$S^{(\alpha)}_{\mathrm{GGE}} = \frac{1}{1-\alpha} \ln \mathrm{Tr}\rho^{\alpha}_{\mathrm{GGE}}, \tag{19}$$

where ρ_{GGE} is defined in (10). We now discuss how to calculate (19) using the thermodynamic Bethe ansatz. Similar to (15), in the thermodynamic limit the GGE Rényi entropies are written as

$$S^{(\alpha)}_{\mathrm{GGE}} = \frac{1}{1-\alpha}\left[\ln \int D\rho\, \exp(-\alpha\mathcal{E}+S_{\mathrm{YY}}) + \alpha f_{\mathrm{GGE}}\right], \tag{20}$$

where $f_{\mathrm{GGE}} \equiv -\ln Z_{\mathrm{GGE}}$, $\mathcal{E}$ is the same as in (16), and S_{YY} is the GGE thermodynamic entropy. The functional integral in (20) can be treated using the saddle-point method. The functional $\mathcal{S}^{(\alpha)}_{\mathrm{GGE}}$ that has to be minimized depends explicitly on the Rényi index α, and it is defined as

$$\mathcal{S}^{(\alpha)}_{\mathrm{GGE}} \equiv -\alpha\mathcal{E} + S_{\mathrm{YY}}. \tag{21}$$

The saddle-point condition leads to the modified TBA equations for $\eta^{(\alpha)}_n$ as

$$\ln \eta^{(\alpha)}_n = \alpha g_n + \sum_{m=1}^{\infty} a_{nm} \star \ln\left[1+1/\eta^{(\alpha)}_m(\lambda)\right]. \tag{22}$$

The particle densities $\rho^{(\alpha)}_n$ are obtained by substituting $\eta^{(\alpha)}_n$ in the Bethe equations (5). By combining (21) and (19), one obtains that the density of the Rényi entropies for a GGE is

$$S^{(\alpha)}_{\mathrm{GGE}} = \frac{1}{1-\alpha}[(-\alpha\mathcal{E}+S_{\mathrm{YY}})|_{\rho^{(\alpha)}_n} + \alpha f_{\mathrm{GGE}}|_{\rho^{(1)}_n}], \tag{23}$$

where $\rho^{(1)}_n$ is the saddle-point density for $\alpha = 1$ that describes local steady-state properties.

As it is clear from (22), the macrostate describing the Rényi entropies depends on α. This is surprising because both the Rényi entropies and the von Neumann entropy are calculated from the same quantum state. An interesting consequence is that the region of energy spectrum of the post-quench Hamiltonian that is relevant for describing the Rényi entropies is different from that describing the local observables. A similar behavior happens for nonintegrable models, where it is a consequence of the eigenstate thermalization hypothesis [137].

At this point, it is important to stress that the method to calculate the Rényi entropies that we outlined so far requires as crucial ingredient the set of infinitely many Lagrange multipliers β_k entering in the driving functions g_n [cf. (13)]. Fixing the β_k by using the constraint (11) is a formidable task that cannot be carried out in practice. However, this difficulty can be overcome in two ways. One is to use the quench action method [138,139]. The quench action provides direct access to the thermodynamic macrostate describing the stationary state. The driving functions g_n are extracted from the overlaps between the initial state and the eigenstates of the post-quench Hamiltonian, without relying on the β_k. Interestingly, a subset of the thermodynamically relevant overlaps is sufficient to determine the macrostate (see [140–142]). For a large class of initial states, the overlaps can be determined analytically [143–158]. This holds also for systems in the continuum, such as the Lieb-Liniger gas. For instance, in Refs. [147–149,159], the overlaps between the Bose condensate (BEC) state and the eigenstates of the Lieb-Liniger model have been calculated, for both attractive and repulsive interactions. Interestingly, a crucial feature of all the initial states for which it has been possible to calculate the overlaps is reflection symmetry. Reflection-symmetric initial states have nonzero overlap only with parity-invariant eigenstates, which are identified by solutions of the Bethe equations containing only pairs of rapidities with opposite sign, i.e., such that $\{\lambda_j\} = \{-\lambda_j\}$. Interestingly, the role played by parity invariance for the solvability of quantum quenches has been investigated in Ref. [160] for lattice models and in Ref. [161] for integrable field theories. Also, one should remark that non-reflection-symmetric initial states have been found [158] for which the quench action method can be applied. We should mention that the knowledge of the overlaps was crucial in Ref. [41] to obtain the steady-state Rényi entropies after the quench from the Néel state. For some quenches, the TBA

macrostates describing the steady state can be derived from the expectation values of the conserved quantities over the initial state, without knowing the overlaps [136]. For instance, this is the case for the quench from the tilted Néel state [162] (see, however, Ref. [144] for a recent conjecture for the overlaps). In these cases, one can use the TBA equations (18) to extract the driving functions g_n from the macrostate densities. The functions g_n can then be used in the generalized TBA equations (22) to derive the Rényi entropies. The validity of this approach for homogeneous quenches has been investigated recently in Ref. [42]. Crucially, for quenches from piecewise homogeneous initial states, the GGE macrostate describing the local steady state is determined by solving a continuity equation (see below), and the TBA driving functions are not even defined. This implies that the approach of Ref. [42] has to be employed.

D. Min entropy of the GGE

Before proceeding, it is interesting to consider the limit $\alpha \to \infty$ of the GGE Rényi entropies, which corresponds to min entropy of the GGE, or the so-called single-copy entanglement entropy $S^{(\infty)}$, which is written in terms of the largest eigenvalues λ_M of the reduced density matrix as $S^{(\infty)} = -\ln \lambda_M$. For homogeneous quenches in the XXZ chain, the steady-state value of the single-copy entanglement has been derived in Ref. [40]. An interesting feature is that the thermodynamic macrostate that determines its steady-state value has zero Yang-Yang entropy (see Ref. [42] for a discussion of some general conditions for this to hold true). Moreover, for quenches in the strong anisotropy limit of the XXZ chain (see Sec. IV A for its definition), this macrostate is the ground state of the chain. Notice that the ground state of the XXZ chain does not contain bound states. This picture breaks down at sufficiently small values of the chain anisotropy, where $S^{(\infty)}$ is described by a different macrostate. This new macrostate has zero Yang-Yang entropy and the associated TBA densities $\rho_n^{(\infty)}$ exhibit a Fermi-sea structure [40], but it has a nontrivial bound-state content.

We now discuss the TBA derivation of the steady-state value of the min entropy after a homogeneous quenches. The generalization to quenches from piecewise homogeneous initial states is straightforward. First, it is useful to rewrite the TBA densities $\eta_n^{(\alpha)}$ [cf. (22)] as [41]

$$\eta_n^{(\alpha)} = \exp(\alpha \gamma_n). \tag{24}$$

Here, the functions γ_n have to be determined by using the TBA equations (22). Clearly, from (24) one has that in the limit $\alpha \to \infty$, $\eta_n^{(\alpha)}$ (vanish) diverge for $(\gamma_n < 0)\ \gamma_n > 0$. Using (24), the TBA equations (22) for $\eta_n^{(\alpha)}$ now read as

$$\alpha\gamma_n = \alpha g_n + \sum_m \int d\mu\, a_{nm}(\mu-\lambda) \times \ln\{1+\exp[-\alpha\gamma_m(\mu)]\}. \tag{25}$$

In the limit $\alpha \to \infty$, the last term in (25) is nonzero only for $\gamma_m < 0$, and it becomes linear in α. This allows one to rewrite (25) as

$$\gamma_n = g_n + \sum_m \int d\mu\, a_{nm}(\mu-\lambda)\gamma_m^+(\mu), \tag{26}$$

where we defined γ_n^+ as

$$\gamma_n^+ \equiv \begin{cases} \gamma_n & \text{if} \quad \gamma_n < 0, \\ 0 & \text{if} \quad \gamma_n > 0. \end{cases} \tag{27}$$

Notice that, as it is clear from the definition (27), the integral equations in (26) are nonlinear. After solving (26), the particle densities $\rho_n^{(\infty)}$ are obtained by using the TBA equations (5).

One obtains that $\rho_n^{(\infty)}$ are nonzero only for λ such that $\gamma_n < 0$. This happens because the $\rho_n^{(\infty)}$ cannot diverge, whereas from (24), one has that $\eta_n^{(\infty)}$ diverge for λ such that $\gamma_n > 0$. More quantitatively, in the limit $\alpha \to \infty$ the system (5) becomes

$$2\pi\rho_n = a_n - \sum_{m=1}^{\infty} \int d\mu\, a_{nm}(\mu-\lambda)\rho_m(\mu)\theta_H(-\gamma_m), \tag{28}$$

where, again, ρ_n is nonzero only for λ such that $\gamma_n < 0$. The equation for the hole density $\rho_n^{(h)}$ is given as

$$2\pi\rho_n^{(h)} = a_n - \sum_{m=1}^{\infty} \int d\mu\, a_{nm}(\mu-\lambda)\rho_m(\mu)\theta_H(-\gamma_m). \tag{29}$$

Notice that (29) is the same as (28), although the support, i.e., the values of λ for which ρ_n and $\rho_n^{(h)}$ are nonzero, is different. In fact, the supports of particle and hole densities are complementary. By using (9), it is straightforward to check that this implies that the Yang-Yang entropy is zero. Finally, by taking the limit $\alpha \to \infty$ in (23), one obtains that

$$S_{\rm GGE}^{(\infty)} = \mathcal{E}|_{\rho_n^{(\infty)}} + L\, f_{\rm GGE}|_{\rho_n^{(1)}}, \tag{30}$$

where $\rho_n^{(1)}$ is the macrostate describing (quasi)local observables in the steady state. Apart from the contribution of the GGE grand-canonical potential $f_{\rm GGE}$, the min entropy is determined by the driving $\mathcal{E}$ only. Also, for quenches that can be treated with the quench action, one has $f_{\rm GGE} = 0$, due to the normalization of the overlaps [140], which further simplifies (30).

III. OBTAINING THE RÉNYI ENTROPIES IN GHD

Here, we discuss the GHD approach to calculate the steady-state Rényi entropies in Sec. III A (see Refs. [103,104]), focusing on the entropies in Sec. III B.

A. Generalized hydrodynamics (GHD)

Let us consider the setup that is depicted in Fig. 1. After the quench, information spreads ballistically from the interface between A and B. At long times, local and quasilocal quantities depend only on the ratio $\zeta = x/t$, with t the time after the quench and x the distance from the interface between A and B. A remarkable result is that in the scaling limit of long times and large distances, for each fixed ray ζ, dynamical properties of the system are described by a GGE [103,104]. Similar to homogeneous quenches, this GGE is identified by a thermodynamic macrostate (see Sec. II B), i.e., by a set of particle and hole densities $\rho_{\zeta,n}$ and $\rho_{\zeta,n}^{(h)}$. For $\zeta = 0$ the macrostate identifies the so-called nonequilibrium steady state (NESS). We anticipate that the NESS is the relevant macrostate for describing the steady-state Rényi entropies of a subsystem placed at the interface between A and B. Clearly, deep in the bulk of the

two chains, i.e., for $x/t \to \pm\infty$, the steady state is the same as that arising after the homogeneous quenches with initial states $|\Psi_A\rangle$ and $|\Psi_B\rangle$. Let us denote as $\rho_{\pm\infty,n}$ the macrostates that describe these steady states.

The central result of the generalized hydrodynamics [103,104] is that for generic $\zeta = x/t$, the macrostate $\rho_{\zeta,n}$ satisfies a continuity equation having $\rho_{\pm\infty,n}$ as boundary conditions for $\zeta \to \pm\infty$. The continuity equation is conveniently written in terms of the filling functions $\vartheta_{\zeta,n}$ [cf. (4)] as

$$[\zeta - v_{\zeta,n}(\lambda)]\partial_\zeta \vartheta_{\zeta,n}(\lambda) = 0, \tag{31}$$

where $v_{\zeta,n}$ are the group velocities of the low-lying (particle-hole) excitations around $\rho_{\zeta,n}$. Crucially, in (31) there is no explicit scattering term between different quasiparticles. This is a consequence of integrability. Indeed, for interacting integrable models, the full effect of interactions is taken into account by the renormalization of the group velocity $v_{\zeta,n}$. The TBA calculation of $v_{\zeta,n}$ will be illustrated below. Notice that in Eq. (31) each ray ζ can be treated separately. The general solution of (31) can be written as [103,104]

$$\vartheta_{\zeta,n}(\lambda) = \theta_H(v_{\zeta,n} - \zeta)(\vartheta_{+\infty,n} - \vartheta_{-\infty,n}) + \vartheta_{-\infty,n}. \tag{32}$$

Here, θ_H is the Heaviside theta function and $\vartheta_{\pm\infty,n}$ are the boundary conditions in the limits $\zeta \to \pm\infty$. Again, they identify the macrostates describing the steady state after the quenches from $|\Psi_A\rangle$ and $|\Psi_B\rangle$ (see Fig. 1), respectively. Notice that the solution (32) is only implicit because the velocities $v_{\zeta,n}$ have to be determined self-consistently. The equations that determine the particle density $\rho_{\zeta,n}$ are the same as in (5). In terms of $\vartheta_{\zeta,n}$ they read as

$$2\pi\rho_{\zeta,n}\vartheta_{\zeta,n}^{-1} = a_n - \sum_{m=1}^{\infty} a_{nm} \star \rho_{\zeta,m}, \tag{33}$$

where $\vartheta_{\zeta,n}$ are obtained from (32).

As anticipated, the crucial ingredients of the GHD are the group velocities $v_{\zeta,n}$. In the Bethe ansatz framework, these are constructed as particle-hole excitations above $\rho_{\zeta,n}$. For generic integrable *interacting* models, the effect of particle-hole excitations is to renormalize ("dress") the quasiparticle rapidities. This is reflected in a renormalization of the quasiparticle energies and group velocities.

In the following, we describe how to calculate this renormalization by using the approach described in Ref. [163]. We denote the "dressed" single-particle energies by $e_{\zeta,n}$, whereas the "bare" ones are denoted by ϵ_n. In terms of $e_{\zeta,n}$, the group velocities $v_{\zeta,n}$ are written as [163]

$$v_{\zeta,n} = \frac{e'_{\zeta,n}}{2\pi\rho^{(t)}_{\zeta,n}}. \tag{34}$$

Here, $e'_{\zeta,n} \equiv de_{\zeta,n}/d\lambda$, and $\rho_n^{(t)}$ is the total density of the thermodynamic macrostate. The functions $e'_{\zeta,n}$ are obtained by solving the system of nonlinear integral equations [163]

$$e'_{\zeta,n} - \epsilon'_n + \frac{1}{2\pi}\sum_m \int d\mu\, e'_{\zeta,m}(\mu) a_{nm}(\mu - \lambda)\vartheta_{\zeta,m}(\mu) = 0. \tag{35}$$

Here, a_{nm} is the same scattering matrix as in the TBA equations (5), and we defined $\epsilon'_n \equiv d\epsilon_n/d\lambda$. A very efficient strategy to solve (31) and (35) is by iteration: one starts with an initial guess for $v_{\zeta,n}$, using (32) to derive $\vartheta_{\zeta,n}$. Thus, a new set of velocities is determined by using (34) and (35). These two steps are iterated until convergence is reached.

B. GHD approach for Rényi entropies

Here, we consider a finite subsystem A' of length ℓ at the interface between A and B (see Fig. 1). We are interested in the steady-state value of the Rényi entropy density $S^{(\alpha)}/\ell$ of A' for generic α. For $\alpha = 1$ the result has been provided in Ref. [40]. The key idea is that for any finite ℓ, in the limit $t \to \infty$, the density of Rényi entropy has to coincide with that of the Rényi entropy of the GGE that describes the local equilibrium state. Now, in the limit $t \to \infty$ any finite region around the interface between A and B is described by the GGE with $\zeta = 0$.

The general idea to obtain the steady-state Rényi entropies is to combine the GHD framework (see Sec. III A) with the TBA method for the Rényi entropies (see Sec. II C). The densities $\vartheta_{\zeta=0,n}$ are obtained by solving the GHD continuity equations (31). Then, the Rényi entropies are obtained using the TBA method described in Sec. II. Crucially, the second step requires knowing the driving g_n [see (18) for its definition] that determines $\eta_n^{(\alpha)}$. In contrast with homogeneous quenches, g_n is not known *a priori*. Here, following Ref. [42], g_n is extracted from the TBA equations (18), by substituting the densities $\vartheta_{\zeta=0,n}$ obtained from (31). Finally, g_n is used in the TBA equations (22) and (5) to obtain the densities $\eta_n^{(\alpha)}$ and $\rho_n^{(\alpha)}$. The final expression for the Rényi entropies' densities is given by (23).

IV. ANALYTICAL RESULTS FOR THE XXZ CHAIN

In this section, by using the approach presented in Sec. III, we calculate the steady-state Rényi entropies after a quench from a piecewise homogeneous initial state in the XXZ chain. Section IV A introduces the XXZ and the quench protocol, in particular, the *expansion quench*. The GHD solution of the expansion quench is detailed in Secs. IV B, IV C, and IV D. Finally, in Sec. IV E we present our analytical predictions for the entropies.

A. Model and quench protocols (expansion quench)

The spin-$\frac{1}{2}$ XXZ chain is defined by the Hamiltonian

$$H = \sum_{i=1}^{L}\left[\tfrac{1}{2}\left(S_i^+ S_{i+1}^- + S_i^- S_{i+1}^-\right) + \Delta S_i^z S_{i+1}^z\right], \tag{36}$$

where $S_i^{+,-,z}$ are spin-$\frac{1}{2}$ operators and Δ is the anisotropy parameter. We consider periodic boundary conditions by identifying sites 1 and $L+1$ of the chain. We restrict ourselves to $\Delta > 1$. In the generic quench protocol, at $t = 0$ the two chains A and B (see Fig. 1) are prepared in two macroscopically different states Ψ_A and Ψ_B. At $t > 0$, the unitary dynamics under the XXZ Hamiltonian (36) is investigated. Here, we also consider a special type of quench, which we term *expansion quench*. In the expansion quench part A (see Fig. 1) is prepared in the vacuum state of the quasiparticles, which for the XXZ chain is the ferromagnetic state with all the spins

pointing up, i.e.,

$$|F\rangle \equiv |\uparrow\uparrow\uparrow\ldots\rangle. \tag{37}$$

After mapping the XXZ chain onto a system of interacting fermions, the expansion quench is equivalent to a box-trap expansion, which is routinely used in cold-atom experiments. Here, we only consider the expansion of the Néel state $|N\rangle$ and of the Majumdar-Ghosh (or dimer) state $|\mathrm{MG}\rangle$. The Néel state is defined as

$$|N\rangle \equiv \frac{1}{\sqrt{2}}(|\uparrow\downarrow\uparrow\ldots\rangle + |\downarrow\uparrow\downarrow\ldots\rangle). \tag{38}$$

The Majumdar-Ghosh state (dimer state) is defined as

$$|\mathrm{MG}\rangle \equiv \frac{1}{2^{\frac{L}{4}}}(|\uparrow\downarrow\rangle - |\downarrow\uparrow\rangle)(|\uparrow\downarrow\rangle - |\downarrow\uparrow\rangle)\ldots. \tag{39}$$

B. GHD solution of the expansion quench

It is interesting to discuss the solution of the expansion quench in the XXZ chain by using the framework of the generalized hydrodynamics (GHD) (see Sec. III A). Since part A of the system is prepared in the vacuum, a major simplification is that

$$\vartheta_{+\infty,n}(\lambda) = 0,\ \forall\ \lambda. \tag{40}$$

This has striking consequences in the continuity equation (31). First, we restrict ourselves to the case $\zeta = 0$, which, as already stressed, is the relevant ray to describe the interface between A and B and the steady-state entropies. By using the general solution (32) of (31), Eq. (40) implies that ϑ_n is written as

$$\vartheta_n(\lambda) = \theta_H(v_n)\vartheta_{-\infty,n}, \tag{41}$$

where we omit the subscript ζ since we are focusing on $\zeta = 0$. Clearly, from (41), one has that $\vartheta_n(\lambda)$ is nonzero only for λ such that $v_n(\lambda) > 0$. An important consequence of (41) is that $\vartheta_n(\lambda) = 0$ for λ such that $v_n(\lambda) < 0$. The physical interpretation is that quasiparticles with these rapidities that are originated in B do not reach the interface with A because their group velocities change sign during the dynamics. It is useful to express Eq. (41) in terms of the dressed energies e'_n. By using the definition (34), and the fact that $\rho_n^{(t)}(\lambda) \geqslant 0$, one has

$$v_n(\lambda) > 0 \Leftrightarrow e'_n(\lambda) > 0, \tag{42}$$

which allows one to replace $\theta_H(v_n)$ with $\theta_H(e'_n)$ in (41). An important consequence is that the integral equation for the dressed energy e'_n [cf. (35)] is decoupled from the continuity equation (31), and it becomes

$$0 = \epsilon'_n - e'_n - \frac{1}{2\pi}\sum_m \int d\mu\, e'_m(\mu)a_{nm}(\mu-\lambda)\vartheta_{-\infty,m}(\mu) \times \theta_H(e'_m(\mu)). \tag{43}$$

Here, ϵ'_n is the derivative of the bare energy of the quasiparticles and $\vartheta_{-\infty,n}$ is the macrostate describing local equilibrium in the limit $\zeta \to -\infty$.

C. Absence of bound-state transport after the expansion

An intriguing feature of the expansion quench in the XXZ chain is that, for large enough Δ, there is no bound-state transport between A and B (see Fig. 1). This is a genuine effect of the interactions, which renormalize ("dress") the group velocities of the system quasiparticles. Due to this dressing, the group velocities v_n of the bound states with $n > 1$ that are created in B change sign before reaching the boundary with A. Formally, the reason for this behavior is that for the XXZ chain in the large-Δ limit one has

$$e'_n < 0,\ \forall\ \lambda \quad \text{for} \quad n > 1. \tag{44}$$

In the following, we first illustrate the mechanism by which Eq. (44) implies the absence of bound-state transport at large Δ, and then we discuss its regime of validity upon lowering Δ. Equation (44) implies that in the system of integral equations (43) the equation for $n = 1$ is decoupled from the rest, and it is given as

$$\epsilon'_1 = e'_1 + \frac{1}{2\pi}\int d\mu\, e'_1(\mu)a_{11}(\mu-\lambda) \times \vartheta_{-\infty,1}(\mu)\theta_H(e'_1(\mu)). \tag{45}$$

The derivative e'_n of the dressed energy density for bound states with $n > 1$ is obtained by substituting the solution e'_1 of (45) in (43). This gives

$$e'_n = \epsilon'_n - \frac{1}{2\pi}\int d\mu\, e'_1(\mu)a_{n1}(\mu-\lambda) \times \vartheta_{-\infty,1}(\mu)\theta_H(e'_1(\mu)). \tag{46}$$

Equation (46) has to be used to check (44) self-consistently (see below).

The decoupling of the equation for η_1 in (45) is reflected in a similar behavior for the particle density ρ_1. From Eq. (5), it is clear that Eqs. (44) and (41) imply that $\eta_n \to \infty$ and that $\rho_n \to 0$ for $n > 1$. On the other hand, for $n = 1$, one has that ρ_1 is nonzero only for λ such that $e'_1 > 0$. Specifically, from (5) the finite part of ρ_1 is obtained by solving the integral equation

$$\rho_1(\vartheta_{-\infty,1})^{-1} - \frac{a_1}{2\pi} = -\frac{1}{2\pi}\int d\mu\, a_{11}(\lambda-\mu) \times \rho_1(\mu)\theta_H(e'_1(\mu)). \tag{47}$$

The fact that ρ_n is identically zero for $n > 1$ implies that the bound states with $n > 1$ do not affect the local equilibrium properties at the interface between A and B. Equivalently, the information about the bound states that are created in B does not arrive at the interface with A.

We now discuss the validity of this result as a function of Δ. The strategy is to check (44) by substituting the solution of (45) in (46). This gives the condition

$$\epsilon'_n - \frac{1}{2\pi}\int d\mu\, e'_1(\mu)a_{n1}(\mu-\lambda)\vartheta_{-\infty,1}(\mu)\theta_H(e'_1(\mu)) < 0. \tag{48}$$

We now show that for the expansion quench the condition (48) is satisfied in the XXZ chain with large enough Δ. First, one can verify that the leading order of the bare energy ϵ'_n for large

Δ is given as [135]

$$\epsilon'_n = 2z^{n-1}\sin(2\lambda) + \mathcal{O}(z^{n+1}), \quad \text{with} \quad z \equiv e^{-\eta}. \tag{49}$$

Here, $\eta \equiv \operatorname{arccosh}(\Delta)$. We now assume that $e'_1 = \mathcal{O}(1) > 0$ for some rapidities λ. We also assume that $\vartheta_{-\infty,1} > 0$ and $\vartheta_{-\infty,1} = \mathcal{O}(1)$. These conditions are verified for all the quenches considered in this work. It is also natural to expect that they hold true for a larger class of quenches. Now, using that in the large-Δ limit, $a_{n1} = \mathcal{O}(1)$ and $a_{n1} > 0$, one has that the second term in (48) is $\mathcal{O}(1)$ and negative, whereas the first one can be made arbitrarily small upon increasing Δ [cf. (49)]. This allows us to conclude that Eq. (44) holds true for large enough Δ. Upon lowering Δ, at a certain value Δ_n^* the n-particle bound states start to be transmitted between the two chains. These "critical" Δ_n^* depend on the initial state that is released. Furthermore, we observe that, at least for the first few values of n, $\Delta_n^* < \Delta_m^*$ for $n > m$, i.e., larger bound states start to be transmitted at smaller Δ's. Finally, for the initial states that we consider (Néel state and Majumdar-Ghosh state) we notice that $\Delta_1^* < 1.5$.

D. Expansion quench in the large-Δ limit: Exact results

Before discussing the steady-state entropies, it is useful to investigate the large-Δ expansion of the macrostate describing local and quasilocal observables. Here, we focus on the expansion of the Néel state and the Majumdar-Ghosh state.

1. Expanding the Néel state

By using (41) and the fact that for the Néel state in the limit $\Delta \to \infty$ one has that [140] $\vartheta_{-\infty,1} \to 1$, one obtains that ϑ_1 becomes a step function. Precisely, one has

$$\vartheta_1 = \theta_H(e'_1(\lambda)). \tag{50}$$

Equation (49) and the fact that $a_{11} = 2$ at the leading order in $1/\Delta$ imply that the dressed energy e'_1 is obtained by solving the integral equation [cf. (43)]

$$e'_1 = 2\,\sin(2\lambda) - \frac{1}{\pi}\int d\mu\, e'_1(\mu)\theta_H(e'_1(\mu)). \tag{51}$$

Equation (51) implies that

$$e'_1 = 2\,\sin(2\lambda) + \gamma, \tag{52}$$

with γ to be determined. After substituting (52) in (51) one obtains an equation for γ as

$$2\,\sin(2\lambda) + \gamma = 2\,\sin(2\lambda) - \frac{1}{\pi}\int_{\lambda_-}^{\lambda_+} d\mu[2\,\sin(2\lambda) + \gamma], \tag{53}$$

where we defined

$$\lambda_- = -\frac{1}{2}\arcsin\left(\frac{\gamma}{2}\right), \tag{54}$$

$$\lambda_+ = \frac{\pi}{2} + \frac{1}{2}\arcsin\left(\frac{\gamma}{2}\right). \tag{55}$$

By performing the integral in (53), one obtains that γ is the solution of

$$\frac{1}{\pi}\left[\sqrt{4-\gamma^2} + \gamma\,\arccos\left(\frac{\gamma}{2}\right)\right] + \gamma = 0. \tag{56}$$

Equation (56) cannot be solved analytically. From (56) one obtains numerically $\gamma \approx -0.3989$.

We now determine the particle density ρ_1. First, by using the TBA Eq. (47) together with (50), one has that ρ_1 is zero for $\lambda \notin [\lambda_-, \lambda_+]$. For $\lambda \in [\lambda_-, \lambda_+]$, ρ_1 is obtained by solving

$$\rho_1 - \frac{1}{\pi} + \frac{1}{\pi}\int_{\lambda_-}^{\lambda_+} d\mu\,\rho_1 = 0, \tag{57}$$

where we used the TBA Eq. (47), and that at the leading order in $1/\Delta$ one has $a_1 = 2$. From (57), one has that ρ_1 exhibits a Fermi-sea structure, and it is given as

$$\rho_1 = \begin{cases} [\pi + \lambda_+ - \lambda_-]^{-1} & \text{if } \lambda \in [\lambda_-, \lambda_+], \\ 0 & \text{otherwise.} \end{cases} \tag{58}$$

On the other hand, the hole density $\rho_1^{(h)}$ is nonzero only for $\lambda \notin [\lambda_-, \lambda_+]$, where $\rho_1^{(h)} = [\pi + \lambda_+ - \lambda_-]^{-1}$. The fact that the hole and the particle density have complementary support implies that in the limit $\Delta \to \infty$, the Yang-Yang entropy is vanishing.

2. Expanding the Majumdar-Ghosh state

A similar expansion can be obtained for the expansion of the Majumdar-Ghosh state. In contrast with the Néel state (see Sec. IV D 1), at the leading order in $1/\Delta$ one now has $\vartheta_{-\infty,1} = \cos^2(\lambda)$. The leading order in $1/\Delta$ of the dressed energy e'_1 [cf. (45)] is now obtained by solving

$$e'_1 = 2\,\sin(2\lambda) - \frac{1}{\pi}\int d\mu\, e'_1(\mu)\cos^2(\mu)\theta_H(e'_1(\mu)). \tag{59}$$

Equation (59) implies that

$$e'_1 = 2\,\sin(2\lambda) + \gamma', \tag{60}$$

where γ' is obtained by solving

$$\frac{1}{2\pi}\left[\sqrt{4-\gamma'^2} + \gamma'\arccos\left(\frac{\gamma'}{2}\right)\right] + \gamma' = 0. \tag{61}$$

Equation (61) gives $\gamma' \approx -0.2487$. Equation (61) is the same as (56), apart from a factor $\frac{1}{2}$ in the first term. The TBA equation (47) for the particle density ρ_1 is

$$\frac{\rho_1}{\cos^2(\lambda)} - \frac{1}{\pi} + \frac{1}{\pi}\int d\mu\,\rho_1(\mu)\theta_H(e'_1(\mu)) = 0. \tag{62}$$

This implies that $\rho_1 = \gamma''\cos^2(\lambda)$. From (62) the constant γ'' is obtained as

$$\gamma'' = \left[\frac{5}{4}\pi - \frac{1}{2}\arcsin\left(\frac{\gamma'}{2}\right)\right]^{-1}, \tag{63}$$

where γ' is the solution of (61). Finally, the result for ρ_1 is written as

$$\rho_1 = \begin{cases} \cos^2(\lambda)\left[\frac{7}{4}\pi - \lambda_+ + \lambda_-\right]^{-1} & \text{if } \lambda \in [\lambda'_-, \lambda'_+], \\ 0 & \text{otherwise,} \end{cases} \tag{64}$$

where we defined

$$\lambda'_- = -\frac{1}{2}\arcsin\left(\frac{\gamma'}{2}\right), \tag{65}$$

$$\lambda'_+ = \frac{\pi}{2} + \frac{1}{2}\arcsin\left(\frac{\gamma'}{2}\right). \tag{66}$$

Notice that $\lambda'_\pm$ coincide with $\lambda_\pm$ [cf. (54) and (55)] after the substitution $\gamma' \to \gamma$. Clearly, in contrast with the Néel state (see Sec. IV D 1), ρ_1 is not a step function.

E. Rényi entropies after the expansion quench

We now calculate the steady-state entropies after the expansion quench. We restrict ourselves to $\Delta > \Delta_2^*$ (see Sec. IV C), which allows us to neglect the contribution of the multispin bound states with $n > 1$.

As described in Sec. III B, the first step is to determine the driving functions g_n [see Eqs. (18) and (22)]. Here, g_n is obtained by first solving (43) for e'_n and then by substituting in

$$g_n = \ln([\vartheta_{-\infty,n}\theta_H(e'_n)]^{-1} - 1) + \sum_m \int d\mu\, a_{nm}(\mu - \lambda) \times \ln[1 - \vartheta_{-\infty,m}(\mu)\theta_H(e'_m)], \tag{67}$$

where we used that for the expansion quench $\vartheta_n = \theta_H(e'_n)\vartheta_{-\infty,n}$.

By using that $e'_n < 0$ for $n > 1$, one obtains that g_n is divergent for any λ for $n > 1$, whereas g_1 diverges for λ such that $e'_1 < 0$, and it is finite otherwise. To derive the Rényi entropies, one has now to solve the TBA equations with the modified driving αg_n. As a consequence of the results outlined above, some simplifications occur. Let us consider the integral equations (22) for $\eta_n^{(\alpha)}$:

$$\ln\left(\eta_n^{(\alpha)}\right) = \alpha g_n + \sum_{m=1}^{\infty} \int d\mu\, a_{nm}(\mu - \lambda) \times \ln\left[1 + 1/\eta_m^{(\alpha)}(\mu)\right]. \tag{68}$$

First, in Eq. (68), the integral in the right-hand side is nonzero only if $\eta_m^{(\alpha)}$ is finite. Thus, from (68), one has that $\eta_n = \alpha g_n$ are divergent for $m > 1$ because g_n are divergent. On the other hand, η_1 is finite for λ such that g_1 is finite, i.e., if $e'_1(\lambda) > 0$ [cf. (67)], and it is divergent otherwise. This implies that the equation for $\eta_1^{(\alpha)}$ is decoupled from the rest and it is given as

$$\ln\left(\eta_1^{(\alpha)}\right) = \alpha g_1\theta_H(e'_1) + \int d\mu\, a_{11}(\mu - \lambda) \times \ln\left[1 + 1/\eta_1^{(\alpha)}(\mu)\theta_H(e'_1)\right]. \tag{69}$$

Here, e'_1 is obtained by solving (45). We now discuss the macrostate densities $\rho_n^{(\alpha)}$. The TBA equations (5) become

$$2\pi\rho_n^{(\alpha)}\left(1 + \eta_n^{(\alpha)}\right) = a_n - \sum_m \int d\mu\, a_{nm}(\mu - \lambda)\rho_m^{(\alpha)}(\mu). \tag{70}$$

Clearly, $\rho_n^{(\alpha)}$ is zero for $n > 1$, reflecting the divergent behavior of $\eta_n^{(\alpha)}$. Also, $\rho_1^{(\alpha)}$ is nonzero only for λ such that $\eta_1^{(\alpha)}$ is finite. To obtain the finite part of $\rho_1^{(\alpha)}$ one has to solve the integral equation

$$2\pi\rho_1^{(\alpha)}\left(1 + \eta_1^{(\alpha)}\right) = a_1 - \int d\mu\, a_{11}(\mu - \lambda)\rho_1^{(\alpha)}(\mu)\theta_H(e'_1). \tag{71}$$

It is interesting to observe that for any finite α, the support of $\rho_1^{(\alpha)}$ does not depend on α, but it is determined by the condition $e'_1 > 0$.

It is now worth making some remarks on the treatment of the single-copy entanglement for $\alpha \to \infty$. Similar to finite α, one has to determine the TBA density $\eta_1^{(\infty)}$. The ansatz (24) becomes

$$\eta_1^{(\alpha)} = \exp(\alpha\gamma_1), \tag{72}$$

where the function γ_1 has to be determined. One has that in the limit $\alpha \to \infty$, Eq. (26) becomes

$$\gamma_1 = g_1 - \int d\mu\, a_{11}(\mu - \lambda)\gamma_1^+(\mu), \tag{73}$$

where γ_1^+ is defined in (27). The particle density $\rho_1^{(\infty)}$ [cf. (28)] becomes

$$2\pi\rho_1^{(\infty)} = a_1 - \int d\mu\, a_{11}(\mu - \lambda)\rho_1^{(\infty)}(\mu)\theta_H(-\gamma_1). \tag{74}$$

The nonzero part of $\rho_1^{(h,\infty)}$ is obtained by using (29).

F. Numerical TBA results

We now provide exact numerical results for the steady-state entropies after the quench from a piecewise homogeneous initial state in the XXZ chain.

1. Macrostate densities and "critical" anisotropies

Numerical results for the macrostate densities $\vartheta_n^{(\alpha)}$ and $\rho_n^{(\alpha)}$ are shown in Fig. 2, for the expansion quenches of the Néel state and of the Majumdar-Ghosh state (first and second columns, respectively), and for the quench from $|N \otimes \mathrm{MG}\rangle$ (third column in Fig. 2). For the expansion quenches we restrict ourselves to $\Delta > \Delta_2^*$ (see Sec. IV C for its definition). As it has been already discussed, this implies that only the densities $\vartheta_1^{(\alpha)}$ and $\rho_1^{(\alpha)}$ are nonzero. For $|N \otimes \mathrm{MG}\rangle$ we show only results for $n = 1$, although all the densities with $n > 1$ are nonzero. Also, one should observe that for the expansion quenches the densities are nonzero only in a subset of $[-\pi/2, \pi/2]$, whereas for $|N \otimes \mathrm{MG}\rangle$ they are nonzero in the full interval $[-\pi/2, \pi/2]$. Finally, as it is clear from Fig. 2(c), ϑ_1 exhibits a quite weak dependence on α.

It is interesting to extract the "critical" anisotropies Δ_n^* for the expansion quenches. Here, we focus on Δ_2^*. As we discussed in Sec. IV C, for $\Delta > \Delta_2^*$ one has that $e'_2 < 0$, giving $\vartheta_2^{(\alpha)} = 0$, which implies that transport of the two-particle bound states between A and B is absent. Formally, Δ_2^* is the point at which e'_2 becomes positive. This is discussed in Fig. 3 showing e'_2 as a function of λ, for the expansion of the Néel state and the Majumdar-Ghosh state. For the Néel state [Fig. 3(a)], one has that for any λ, $e'_2 < 0$ for $\Delta \gtrsim 1.4$, whereas $e'_2 > 0$ for $\Delta = 1.3$, which suggests that $1.3 \gtrsim \Delta_2^* \lesssim 1.4$. For the Majumdar-Ghosh state, one has much smaller values for Δ_2^*. Indeed, from Fig. 3(b) it is clear that $\Delta_2^* < 1.1$. The same analysis could be performed for the three-particle

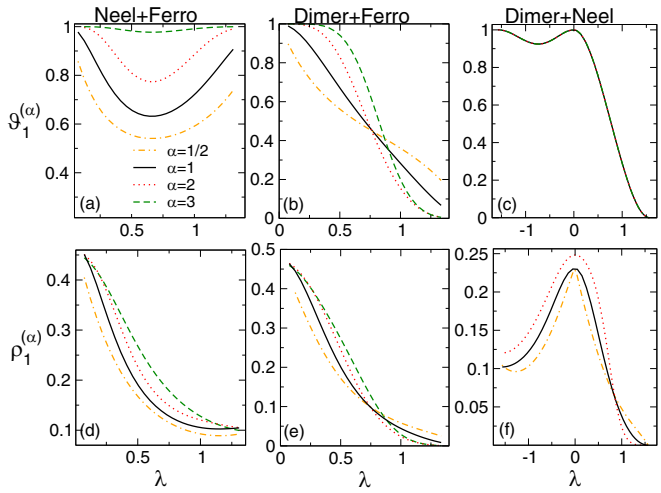

FIG. 2. Rényi entropies after a quench from a piecewise homogeneous initial state in the XXZ chain. Filling function $\vartheta_1^{(\alpha)}$ and particle density $\rho_1^{(\alpha)}$ [panels (a)–(c) and (d) and (e), respectively] describing steady-state Rényi entropies. On the x axis λ is the quasiparticle rapidity. Panels in different columns correspond to quenches from different initial states. All the results are for $\Delta = 2$. For the expansion quenches [panels (a) and (b) and (d) and (e)], only the $n = 1$ string densities are nonzero. For the quench from the state $|N \otimes \mathrm{MG}\rangle$ higher strings contribute (not reported in the figure).

bound states, i.e., for $n = 3$. One should expect a new "critical" anisotropy $\Delta_3^* \leqslant \Delta_2^*$. For $\Delta < \Delta_3^*$ transport of the two-particle and three-particle bound states is permitted. We numerically observed that $e_3 \ll e_2$ for $\Delta < \Delta_2^*$, suggesting that there is an extended region in Δ where only transport of two- and three-particle bound states is allowed. It is natural to expect that a similar scenario occurs for larger bound states, i.e., that there are a "cascade" of transition points $\Delta_1^* > \Delta_2^* > \Delta_3^* > \Delta_4^* \ldots$. This would lead to the intriguing scenario in which transport of larger and larger bound states is activated at smaller and smaller anisotropies.

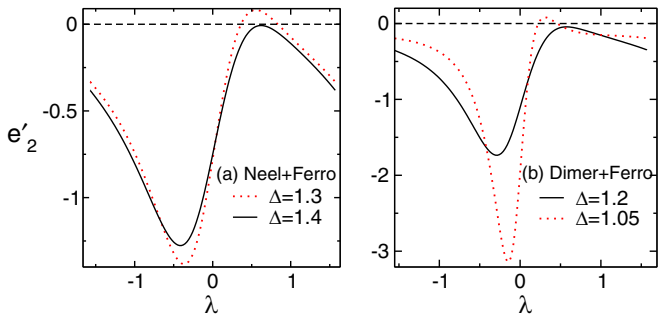

FIG. 3. "Critical" anisotropies Δ_2^* for the two-particle transport after a piecewise homogeneous quench in the XXZ chain. The two panels are for the expansion of the Néel and the Majumdar-Ghosh states. The figure shows the derivative of dressed energy e_2' [cf. (35)] for $n = 2$, plotted as a function of λ. For $\Delta > \Delta_2^*$, one has that $e_2' < 0$, $\forall\, \lambda$, which ensures that transport of two-particle bound states is inhibited. Note that $\Delta_2^* \approx 1.4$ and $\Delta_2^* \approx 1.15$ in (a) and (b), respectively.

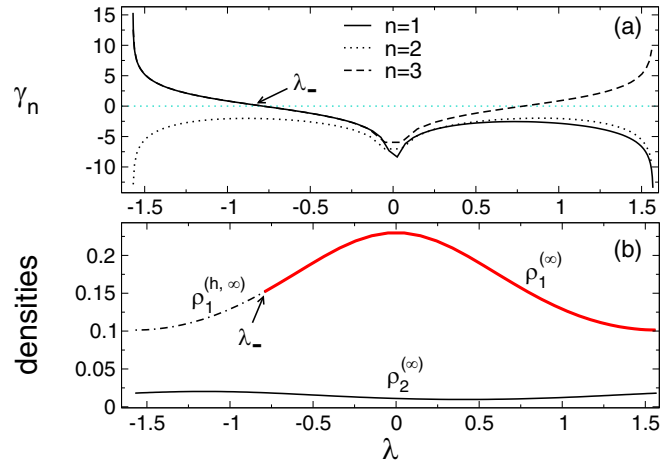

FIG. 4. Min entropy after a piecewise homogeneous quench in the XXZ chain: quench from the state $|N \otimes \mathrm{MG}\rangle$, for $\Delta = 5$. (a) Shows γ_n versus λ for $n \leqslant 3$. Note that $\gamma_2 < 0$ for any λ, in contrast with γ_1 and γ_3. (b) Shows $\rho_n^{(\infty)}$ for $n = 1, 2$. Continuous and dashed-dotted lines denote particle and hole densities, respectively.

Finally, it is useful to consider the limit $\alpha \to \infty$. We focus on the quench from $|N \otimes \mathrm{MG}\rangle$. Figure 4 shows the TBA densities γ_n [see (24) for their definitions], $\rho_n^{(\infty)}$, and $\rho^{(h,\infty)}$ [Figs. 4(a) and 4(b)] plotted as function of λ. Results are for $\Delta = 5$. In Fig. 4(a) we only show results for γ_n with $n \leqslant 3$. Crucially, one has that $\gamma_1 < 0$ for $\lambda > \lambda_-$, with $\lambda_- \approx -0.75$. Similarly, γ_3 is negative in a subinterval of $[-\pi/2, \pi/2]$. On the other hand, one has that $\gamma_2 < 0$ for any $\lambda \in [-\pi/2, \pi/2]$. This is reflected in the behavior of $\rho_n^{(\infty)}$ [Fig. 4(b)].

The continuous lines in Fig. 4(b) are the particle densities $\rho_1^{(\infty)}$ and $\rho_2^{(\infty)}$. The support of $\rho_2^{(\infty)}$ is the full interval $[-\pi/2, \pi/2]$, whereas $\rho_1^{(\infty)}$ is nonzero only for $\lambda > \lambda_-$, with λ_- the same as in Fig. 4(a). The complementary part of the curve (dashed-dotted line) in the panel is the hole density $\rho_1^{(h,\infty)}$.

2. Rényi entropies

The densities reported in Fig. 2 are used to calculate the steady-state entropies by using (23). Figure 5 shows the contributions of the individual quasiparticles to the entropies, plotted versus λ. We report results for the expansion of the Néel state and the Majumdar-Ghosh state [in Figs. 5(a) and 5(b)]. Data for the quench from $|N \otimes \mathrm{MG}\rangle$ and for $n = 1$ and 2 are shown in Figs. 5(c) and 5(d). Notice, however, that for $|N \otimes \mathrm{MG}\rangle$, bound states with $n > 1$ contribute to the Rényi entropies, although we do not report them in the figure. Data in Figs. 5(a) and 5(b) are for the XXZ chain with $\Delta = 2$, while in Figs. 5(c) and 5(d) we consider $\Delta = 5$. While the entropy density for the expansion quenches is positive for all values of λ [see Figs. 5(a) and 5(b)], this is not the case for $|N \otimes \mathrm{MG}\rangle$. The same behavior, i.e., that the density of Rényi entropies is not positive, was observed in homogeneous quenches, and it is the main obstacle when applying the quasiparticle picture to describe the full-time dynamics of the entropies [40,41]. The GHD prediction for the steady-state entropies is obtained by integrating the results in Fig. 5 and by summing over the quasiparticle families. The results are

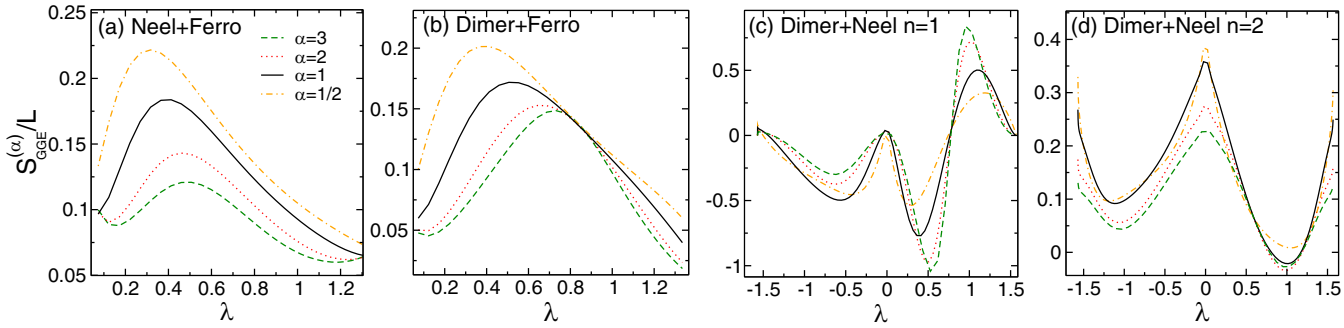

FIG. 5. Steady-state Rényi entropies after the quench from a piecewise homogenous initial state in the XXZ chain: quasiparticle contributions. The entropy density $S^{(\alpha)}_{\rm GGE}/L$ is plotted versus λ, for several values of α. Panels (a) and (b) are for the expansion quench of the Néel state and the Majumdar-Ghosh state, respectively. Data are for $\Delta = 2$. The entropy density is positive for all λ. Panels (c) and (d) show results for the quench from $|N \otimes \mathrm{MG}\rangle$ for $\Delta = 5$. Only results for $n = 1$ and 2 are shown.

reported in Fig. 6 as a function of Δ, and for different initial states. For all the quenches one has that $S^{(\alpha)} < S^{(\alpha')}$, for $\alpha' < \alpha$, as expected. For the expansion of the Néel state, all the Rényi entropies vanish in the large-Δ limit. This reflects that the Néel state is the ground state of the XXZ chain in that limit, similar to the homogeneous case [41]. For the expansion of the Majumdar-Ghosh state, the entropies exhibit a quite weak dependence on Δ. Results for the quench from $|N \otimes \mathrm{MG}\rangle$ are reported in Fig. 6(c). The entropy densities exhibit a decreasing trend upon increasing Δ, although they do not vanish in the limit $\Delta \to \infty$.

V. DMRG RESULTS FOR THE XXZ CHAIN

We now turn to compare the TBA results presented in Sec. IV against tDMRG simulations [164]. We restrict

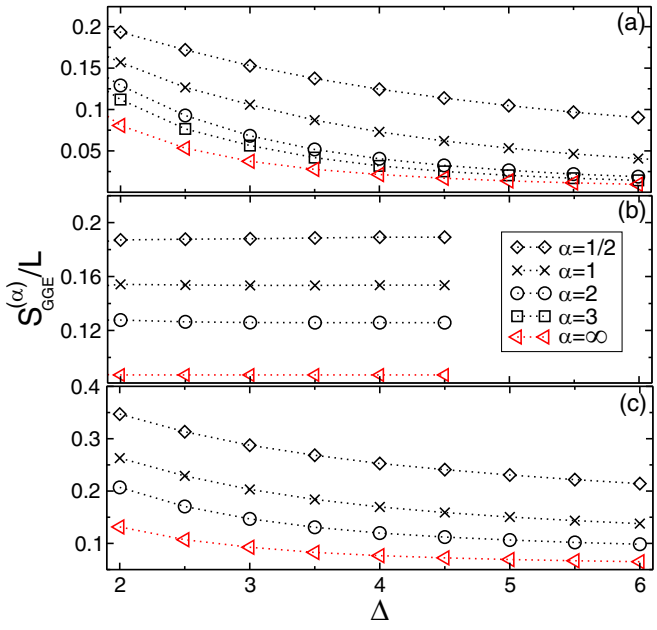

FIG. 6. Steady-state Rényi entropies after a quench from a piecewise homogeneous initial state in the XXZ chain: GHD results for different initial states and Rényi index α. The entropy density $S^{(\alpha)}_{\rm GGE}/L$ is plotted against Δ. In (a) and (b), the triangles correspond to the min entropy ($\alpha \to \infty$).

ourselves to the expansion quenches of the Néel and the Majumdar-Ghosh states, as they are easier to simulate with tDMRG. We employ the framework of the matrix product states (MPS). All the considered initial states admit a simple MPS representation with rather small bond dimension χ. The initial states are time evolved by using a standard second-order Trotter-Suzuki decomposition of the evolution operator e^{-iHt}. The Trotter time discretization step is $\delta t = 0.05$. At each step of the evolution the state loses its MPS form, which has to be restored by performing a singular value decomposition (SVD). To prevent the rapid growth of χ, a truncated SVD is performed with maximum allowed bond dimension $\chi_{\rm max}$. In our simulations we employed $\chi_{\rm max} = 80$. Importantly, here we are interested in calculating the Rényi entropies of a subsystem embedded in the chain (see Fig. 1). In the standard MPS framework, the computational cost for calculating the entropy is $\propto \chi^6$ (see Ref. [165] for the details), in contrast with the cost for calculating the half-chain entropy, which is only $\propto \chi^3$.

Our tDMRG data are reported in Fig. 7 for both the Néel state and of the Majumdar-Ghosh state. The figure shows the entropy density $S^{(\alpha)}/\ell$ versus time. All the results are for the XXZ chain with $L = 40$. Different curves correspond to different values of ℓ. For clarity, we only show results for odd ℓ. Figures 7(a)–7(d) show data for the Néel state and for $\alpha = 2$ and different values of Δ. Figures 7(e)–7(h) show the results for the Majumdar-Ghosh state. Specifically, Figs. 7(e) and 7(f) plot $S^{(2)}/\ell$ for $\Delta = 2$ and $\Delta = 4$, whereas Figs. 7(g) and 7(h) are for $S^{(3)}/\ell$ for the same values of Δ. For the Néel state, the entropy density decreases upon increasing Δ, as expected in the scaling limit (see Fig. 6). Interestingly, sizable oscillations with time are observed, whose amplitude increases with increasing Δ. This is similar to the homogeneous quench from the Néel state [41]. On the other hand, for the Majumdar-Ghosh state, although oscillations with time are present, they decay quite rapidly with increasing ℓ, and their amplitude does not increase upon increasing Δ. The comparison between the Bethe ansatz results for the Rényi entropies is presented in Fig. 8. Panels (a)–(d) show $S^{(\alpha)}/\ell$ for $\alpha = 2, 3$. In all the panels the different symbols are tDMRG data for different values of $\Delta \in [2, 10]$ and $\ell \leqslant 10$. On the x axis we show $1/\ell$. The raw tDMRG data are reported in Fig. 7. The results presented in Fig. 5 are obtained by averaging

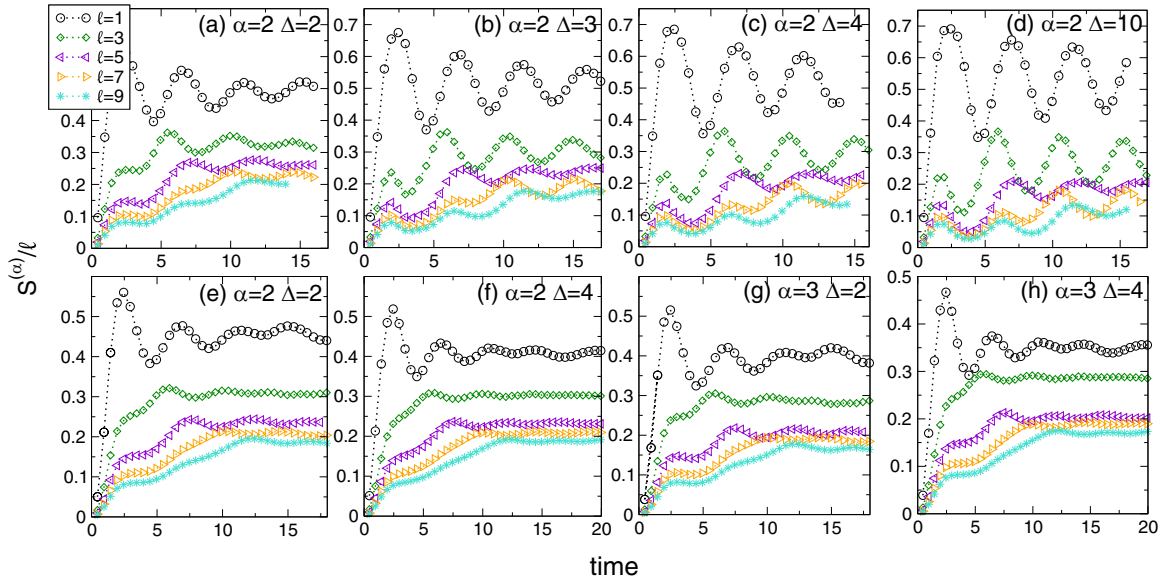

FIG. 7. Steady-state Rényi entropy after the expansion quench of the Néel and the Majumdar-Ghosh states [panels (a)–(d) and (e)–(h), respectively] in the XXZ chain: tDMRG results. The entropy density $S^{(\alpha)}/\ell$ is plotted versus the time after the quench. For the expansion quench of the Néel state [panels (a)–(d)] only $S^{(2)}$ is shown. For the expansion quench of the Majumdar-Ghosh state, (c) and (d) show results for $S^{(2)}/\ell$, whereas (e) and (f) are for $S^{(3)}/\ell$. In all panels different symbols are used for different values of the subsystem size ℓ. Only odd values of ℓ are reported. Notice the large oscillations upon increasing Δ in (a)–(d).

the tDMRG results for $t > 10$, to mitigate the effect of the oscillations with time. The star symbols are the TBA results in the scaling limit (see Fig. 6). Clearly, due to the finite ℓ, corrections are visible. To recover the scaling limit results, we perform a finite-size scaling analysis. The dashed-dotted lines in Fig. 5 are fits to

$$S^{(\alpha)} = \left[s_\infty^{(\alpha)} + \frac{a}{\ell} + \frac{b}{\ell^2} \right] \ell, \tag{75}$$

where $s_\infty^{(\alpha)}$ is the TBA prediction and a, b are fitting parameters. In all the panels, the fits confirm that in the scaling limit the steady-state Rényi entropies are described by the TBA results.

VI. CONCLUSIONS

We investigated the steady-state Rényi entropies after a quench from a piecewise homogeneous initial state in interacting integrable models. Our results were obtained by combining the TBA approach for the Rényi entropies developed in Ref. [40] and the GHD treatment of the quench. We provided explicit results for quenches in the anisotropic Heisenberg XXZ chain from several initial states. We benchmarked our results against tDMRG simulations, finding always satisfactory agreement. We also investigated the steady-state entropies after the expansion quench, in which one of the two chains is prepared in the vacuum of the model excitations. Interestingly, we observed that for large enough anisotropy, the transport of multispin bound states is not allowed. This is reflected in the steady-state entropies, which do not contain

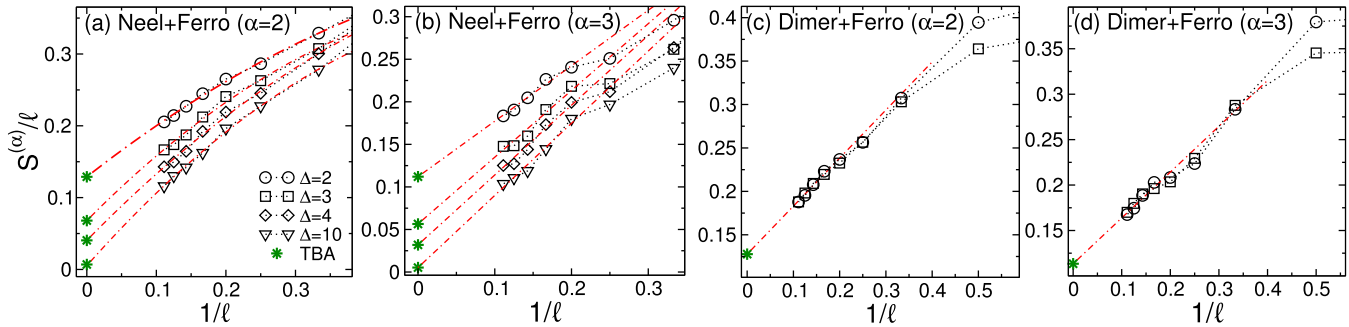

FIG. 8. Steady-state Rényi entropies after a quench from a piecewise homogeneous initial state in the XXZ chain: comparison between theory and tDMRG simulations. Panels (a) and (b) are for the expansion of the Néel state for $\alpha = 2$ and 3, respectively. In all panels $S^{(\alpha)}/\ell$ is plotted versus $1/\ell$, with ℓ the subsystem size. The star symbols are the TBA predictions in the scaling limit. The dashed-dotted lines are fits to $S^{(\alpha)}/\ell = s_\infty^{(\alpha)} + a/\ell + b/\ell^2$, with a, b fitting parameters and $s_\infty^{(\alpha)}$ fixed by the TBA result. Panels (c) and (d): same as in (a) and (b) for the expansion of the Majumdar-Ghosh state. Data are now for $\Delta = 5$. Notice in (c) and (d) the weak dependence on Δ.

information about the bound states. On the other hand, we showed that there is a "critical" anisotropy below which bound-state transport is allowed.

We now discuss some open problems and possible directions for future work. First, it is important to extend the quasiparticle picture to describe the full-time dynamics of the Rényi entropies after the quench. To this purpose, two main issues appear. First, similar to the von Neumann entropy, describing the full-time dynamics of the Rényi entropies requires determining the trajectories of the quasiparticles as function of time, which implies that rays with $\zeta \neq 0$ have to be considered. This analysis has been performed in Ref. [166] for the von Neumann entropy. A more severe obstacle is that the TBA macrostate that describes the steady-state entropies is not the same as that describing (quasi)local observables and the von Neumann entropy, similar to what happens for homogeneous quenches [41]. This does not provide the correct framework for describing the entropy dynamics because the excitations that are responsible of the entanglement growth are the ones constructed around the steady state. To apply the quasiparticle description to the Rényi entropies, one would first need to express the entropy densities as function of the TBA macrostate that describes the steady state. This, however, is still an open and difficult problem.

It would be also important to extend our analysis to different initial states, such as the tilted Néel state and the tilted ferromagnet. For the latter case, it would be interesting to investigate the effect of the tilting on the bound-state transport between the two chains. Another interesting direction is to consider piecewise homogeneous quenches in continuum systems such as the Lieb-Liniger model, or in the Hubbard chain in the limit of strong interactions [158].

ACKNOWLEDGMENTS

I acknowledge very fruitful discussions with B. Doyon. I am grateful to M. Fagotti and B. Bertini for several discussions on a related project. I thank P. Calabrese for reading the manuscript and for several comments. This work was supported by the European Union's Horizon 2020 research and innovation programme under the Marie Sklodowoska-Curie Grant Agreement No. 702612 OEMBS.

[1] N. Schuch, M. M. Wolf, F. Verstraete, and J. I. Cirac, Entropy Scaling and Simulability by Matrix Product States, Phys. Rev. Lett. **100**, 030504 (2008); N. Schuch, M. M. Wolf, K. G. H. Vollbrecht, and J. I. Cirac, On entropy growth and the hardness of simulating time evolution, New J. Phys. **10**, 033032 (2008).

[2] A. Perales and G. Vidal, Entanglement growth and simulation efficiency in one-dimensional quantum lattice systems, Phys. Rev. A **78**, 042337 (2008).

[3] P. Hauke, F. M. Cucchietti, L. Tagliacozzo, I. Deutsch, and M. Lewenstein, Can one trust quantum simulators? Rep. Prog. Phys. **75**, 082401 (2012).

[4] J. Dubail, Entanglement scaling of operators: A conformal field theory approach, with a glimpse of simulability of long-time dynamics in 1+1d, J. Phys. A: Math. Theor. **50**, 234001 (2017).

[5] P. Calabrese and A. Lefevre, Entanglement spectrum in one dimensional systems, Phys. Rev. A **78**, 032329 (2008).

[6] M. Caraglio and F. Gliozzi, Entanglement entropy and twist fields, J. High Energy Phys. 11 (2008) 076; M. B. Hastings, I. Gonzalez, A. B. Kallin, and R. G. Melko, Measuring Renyi Entanglement Entropy with Quantum Monte Carlo, Phys. Rev. Lett. **104**, 157201 (2010); C.-M. Chung, L. Bonnes, P. Chen, and A. M. Lauchli, Entanglement Spectroscopy using Quantum Monte Carlo, Phys. Rev. B **89**, 195147 (2014).

[7] A. J. Daley, H. Pichler, J. Schachenmayer, and P. Zoller, Measuring Entanglement Growth in Quench Dynamics of Bosons in an Optical Lattice, Phys. Rev. Lett. **109**, 020505 (2012).

[8] R. Islam, R. Ma, P. M. Preiss, M. E. Tai, A. Lukin, M. Rispoli, and M. Greiner, Measuring entanglement entropy in a quantum many-body system, Nature (London) **528**, 77 (2015).

[9] A. M. Kaufman, M. E. Tai, A. Lukin, M. Rispoli, R. Schittko, P. M. Preiss, and M. Greiner, Quantum thermalisation through entanglement in an isolated many-body system, Science **353**, 794 (2016).

[10] T. Brydges, A. Elben, P. Jurcevic, B. Vermersch, C. Maier, B. P. Lanyon, P. Zoller, R. Blatt, and C. F. Roos, Probing entanglement entropy via randomized measurements, arXiv:1806.05747.

[11] M. Rigol, V. Dunjko, V. Yurovsky, and M. Olshanii, Relaxation in a Completely Integrable Many-Body Quantum System: An *Ab Initio* Study of the Dynamics of the Highly Excited States of 1D Lattice Hard-Core Bosons, Phys. Rev. Lett. **98**, 050405 (2007).

[12] A. Bastianello and S. Sotiriadis, Quasi locality of the GGE in interacting-to-free quenches in relativistic field theories, J. Stat. Mech. (2017) 023105.

[13] E. Vernier and A. Cortés Cubero, Quasilocal charges and the complete GGE for field theories with nondiagonal scattering, J. Stat. Mech. (2017) 023101.

[14] V. Alba, Simulating the Generalized Gibbs Ensemble (GGE): A Hilbert space Monte Carlo approach, arXiv:1507.06994.

[15] P. Calabrese and J. Cardy, Quantum quenches in extended systems, J. Stat. Mech. (2007) P06008.

[16] M. Cramer, C. M. Dawson, J. Eisert, and T. J. Osborne, Exact Relaxation in a Class of Nonequilibrium Quantum Lattice Systems, Phys. Rev. Lett. **100**, 030602 (2008).

[17] T. Barthel and U. Schollwöck, Dephasing and the Steady State in Quantum Many-Particle Systems, Phys. Rev. Lett. **100**, 100601 (2008).

[18] M. Cramer and J. Eisert, A quantum central limit theorem for non-equilibrium systems: Exact local relaxation of correlated states, New J. Phys. **12**, 055020 (2010).

[19] P. Calabrese, F. H. L. Essler, and M. Fagotti, Quantum Quench in the Transverse-Field Ising Chain, Phys. Rev. Lett. **106**, 227203 (2011); Quantum quench in the transverse field Ising chain: I. Time evolution of order parameter correlators, J. Stat. Mech. (2012) P07016.

[20] P. Calabrese, F. H. L. Essler, and M. Fagotti, Quantum quenches in the transverse field Ising chain: II. Stationary state properties, J. Stat. Mech. (2012) P07022.

[21] M. A. Cazalilla, Effect of Suddenly Turning on Interactions in the Luttinger Model, Phys. Rev. Lett. **97**, 156403 (2006).

[22] M. A. Cazalilla, A. Iucci, and M.-C. Chung, Thermalization and quantum correlations in exactly solvable models, Phys. Rev. E **85**, 011133 (2012).

[23] D. Fioretto and G. Mussardo, Quantum quenches in integrable field theories, New J. Phys. **12**, 055015 (2010); S. Sotiriadis, D. Fioretto, and G. Mussardo, Zamolodchikov-Faddeev algebra and quantum quenches in integrable field theories, J. Stat. Mech. (2012) P02017.

[24] M. Collura, S. Sotiriadis, and P. Calabrese, Equilibration of a Tonks-Girardeau Gas Following a Trap Release, Phys. Rev. Lett. **110**, 245301 (2013); Quench dynamics of a Tonks-Girardeau gas released from a harmonic trap, J. Stat. Mech. (2013) P09025.

[25] M. Fagotti and F. H. L. Essler, Stationary behavior of observables after a quantum quench in the spin-1/2 Heisenberg XXZ chain, J. Stat. Mech. (2013) P07012.

[26] M. Kormos, M. Collura, and P. Calabrese, Analytic results for a quantum quench from free to hard-core one-dimensional bosons, Phys. Rev. A **89**, 013609 (2014).

[27] S. Sotiriadis and P. Calabrese, Validity of the GGE for quantum quenches from interacting to noninteracting models, J. Stat. Mech. (2014) P07024.

[28] F. H. L. Essler, G. Mussardo, and M. Panfil, Generalized Gibbs ensembles for quantum field theories, Phys. Rev. A **91**, 051602 (2015); On Truncated Generalized Gibbs Ensembles in the Ising Field Theory, J. Stat. Mech. (2017) 013103.

[29] L. Vidmar and M. Rigol, Generalized Gibbs ensemble in integrable lattice models, J. Stat. Mech. (2016) 064007.

[30] B. Pozsgay, E. Vernier, and M. A. Werner, On Generalized Gibbs Ensembles with an infinite set of conserved charges, J. Stat. Mech. (2017) 093103.

[31] E. Ilieveski, J. De Nardis, B. Wouters, J.-S. Caux, F. H. L. Essler, and T. Prosen, Complete Generalized Gibbs Ensembles in an Interacting Theory, Phys. Rev. Lett. **115**, 157201 (2015).

[32] J. Cardy, Quantum quenches to a critical point in one dimension: Some further results, J. Stat. Mech. (2016) 023103.

[33] S. Sotiriadis, Memory-preserving equilibration after a quantum quench in a 1d critical model, Phys. Rev. A **94**, 031605 (2016).

[34] J. Mossel and J.-S. Caux, Generalized TBA and generalized Gibbs, J. Phys. A: Math. Theor. **45**, 255001 (2012).

[35] B. Pozsgay, The generalized Gibbs ensemble for Heisenberg spin chains, J. Stat. Mech. (2013) P07003.

[36] M. Fagotti and F. H. L. Essler, Reduced Density Matrix after a Quantum Quench, Phys. Rev. B **87**, 245107 (2013).

[37] M. Fagotti, M. Collura, F. H. L. Essler, and P. Calabrese, Relaxation after quantum quenches in the spin-1/2 Heisenberg XXZ chain, Phys. Rev. B **89**, 125101 (2014).

[38] T. Langen, S. Erne, R. Geiger, B. Rauer, T. Schweigler, M. Kuhnert, W. Rohringer, I. E. Mazets, T. Gasenzer, and J. Schmiedmayer, Experimental observation of a generalized Gibbs ensemble, Science **348**, 207 (2015).

[39] T. Palmai and R. M. Konik, Quasi-local charges and the Generalized Gibbs Ensemble in the Lieb-Liniger model, Phys. Rev. E **98**, 052126 (2018).

[40] V. Alba and P. Calabrese, Quench action and Renyi entropies in integrable systems, Phys. Rev. B **96**, 115421 (2017).

[41] V. Alba and P. Calabrese, Rényi entropies after releasing the Néel state in the XXZ spin chain, J. Stat. Mech. (2017) 113105.

[42] M. Mestyan, V. Alba, and P. Calabrese, Rényi entropies of generic thermodynamic macrostates in integrable systems, J. Stat. Mech. (2018) 083104.

[43] P. Calabrese and J. Cardy, Evolution of entanglement entropy in one-dimensional systems, J. Stat. Mech. (2005) P04010.

[44] M. Fagotti and P. Calabrese, Evolution of entanglement entropy following a quantum quench: Analytic results for the XY chain in a transverse magnetic field, Phys. Rev. A **78**, 010306 (2008).

[45] V. Alba and P. Calabrese, Entanglement and thermodynamics after a quantum quench in integrable systems, Proc. Natl. Acad. Sci. USA **114**, 7947 (2017).

[46] G. De Chiara, S. Montangero, P. Calabrese, and R. Fazio, Entanglement Entropy dynamics in Heisenberg chains, J. Stat. Mech. (2006) P03001.

[47] V. Eisler and I. Peschel, Entanglement in a periodic quench, Ann. Phys. (Berlin) **17**, 410 (2008).

[48] A. Läuchli and C. Kollath, Spreading of correlations and entanglement after a quench in the Bose-Hubbard model, J. Stat. Mech. (2008) P05018.

[49] H. Kim and D. A. Huse, Ballistic Spreading of Entanglement in a Diffusive Nonintegrable System, Phys. Rev. Lett. **111**, 127205 (2013).

[50] M. G. Nezhadhaghighi and M. A. Rajabpour, Entanglement dynamics in short and long-range harmonic oscillators, Phys. Rev. B **90**, 205438 (2014).

[51] A. Coser, E. Tonni, and P. Calabrese, Entanglement negativity after a global quantum quench, J. Stat. Mech. (2014) P12017.

[52] M. Collura, P. Calabrese, and F. H. L. Essler, Quantum quench within the gapless phase of the spin-1/2 Heisenberg XXZ spin-chain, Phys. Rev. B **92**, 125131 (2015).

[53] M. Fagotti and M. Collura, Universal prethermalization dynamics of entanglement entropies after a global quench, arXiv:1507.02678.

[54] P. Calabrese and J. Cardy, Quantum quenches in 1+1 dimensional conformal field theories, J. Stat. Mech. (2016) 064003.

[55] J. S. Cotler, M. P. Hertzberg, M. Mezei, and M. T. Mueller, Entanglement Growth after a Global Quench in Free Scalar Field Theory, J. High Energy Phys. 11 (2016) 166.

[56] A. S. Buyskikh, M. Fagotti, J. Schachenmayer, F. Essler, and A. J. Daley, Entanglement growth and correlation spreading with variable-range interactions in spin and fermionic tunneling models, Phys. Rev. A **93**, 053620 (2016).

[57] M. Kormos, M. Collura, G. Takács, and P. Calabrese, Real time confinement following a quantum quench to a non-integrable model, Nat. Phys. **13**, 246 (2017).

[58] C. Pascu Moca, M. Kormos, and G. Zarand, Hybrid Semiclassical Theory of Quantum Quenches in One-Dimensional Systems, Phys. Rev. Lett. **119**, 100603 (2017).

[59] C. von Keyserlingk, T. Rakovszky, F. Pollmann, and S. Sondhi, Operator Hydrodynamics, OTOCs, and Entanglement Growth in Systems Without Conservation Laws, Phys. Rev. X **8**, 021013 (2018).

[60] P. Calabrese, Entanglement and thermodynamics in non-equilibrium isolated quantum systems, Physica A (Amsterdam) **504**, 31 (2018).

[61] I. Frerot, P. Naldesi, and T. Roscilde, Multi-Speed Prethermalization in Spin Models with Power-Law Decaying Interactions, Phys. Rev. Lett. **120**, 050401 (2018).

[62] E. Bianchi, L. Hackl, and N. Yokomizo, Linear growth of the entanglement entropy and the Kolmogorov-Sinai rate, J. High Energy Phys. 03 (2018) 025.

[63] L. Hackl, E. Bianchi, R. Modak, and M. Rigol, Entanglement production in bosonic systems: Linear and logarithmic growth, Phys. Rev. A **97**, 032321 (2018).

[64] V. Alba, Entanglement and quantum transport in integrable systems, Phys. Rev. B **97**, 245135 (2018).

[65] B. Bertini, E. Tartaglia, and P. Calabrese, Entanglement and diagonal entropies after a quench with no pair structure, J. Stat. Mech. (2018) 063104.

[66] M. Mestyan, B. Bertini, L. Piroli, and P. Calabrese, Exact solution for the quench dynamics of a nested integrable system, J. Stat. Mech. (2017) 083103.

[67] K. Najafi, M. A. Rajabpour, and J. Viti, Light-cone velocities after a global quench in a noninteracting model, Phys. Rev. B **97**, 205103 (2018).

[68] B. Bertini, M. Fagotti, L. Piroli, and P. Calabrese, Entanglement evolution and generalised hydrodynamics: Noninteracting systems, J. Phys. A **51**, 39LT01 (2018).

[69] M. Collura, M. Kormos, and G. Takacs, Dynamical manifestation of Gibbs paradox after a quantum quench, Phys. Rev. A **98**, 053610 (2018).

[70] Y. O. Nakagawa, M. Watanabe, H. Fujita, and S. Sugiura, Universality in volume law entanglement of pure quantum states, Nat. Commun. **9**, 1635 (2018).

[71] V. Alba and P. Calabrese, Entanglement dynamics after quantum quenches in generic integrable systems, SciPost Phys. **4**, 017 (2018).

[72] S. Sotiriadis and J. Cardy, Inhomogeneous quantum quenches, J. Stat. Mech. (2008) P11003.

[73] D. Bernard and B. Doyon, Energy flow in non-equilibrium conformal field theory, J. Phys. A: Math. Theor. **45**, 362001 (2012).

[74] M. J. Bhaseen, B. Doyon, A. Lucas, and K. Schalm, Far from equilibrium energy flow in quantum critical systems, Nat. Phys. **11**, 509 (2015).

[75] N. Allegra, J. Dubail, J.-M. Stephan, and J. Viti, Inhomogeneous field theory inside the arctic circle, J. Stat. Mech. (2016) 053108.

[76] J. Dubail, J.-M. Stephan, J. Viti, and P. Calabrese, Conformal field theory for inhomogeneous one-dimensional quantum systems: The example of non-interacting Fermi gases, SciPost Phys. **2**, 002 (2017).

[77] J. Dubail, J.-M. Stephan, and P. Calabrese, Emergence of curved light-cones in a class of inhomogeneous Luttinger liquids, SciPost Phys. **3**, 019 (2017).

[78] V. Eisler, F. Igloi, and I. Peschel, Entanglement in spin chains with gradients, J. Stat. Mech. (2009) P02011.

[79] A. De Luca, J. Viti, D. Bernard, and B. Doyon, Nonequilibrium thermal transport in the quantum Ising chain, Phys. Rev. B **88**, 134301 (2013).

[80] T. Sabetta and G. Misguich, Non-equilibrium steady states in the quantum XXZ spin chain, Phys. Rev. B **88**, 245114 (2013).

[81] V. Eisler and Z. Racz, Full Counting Statistics in a Propagating Quantum Front and Random Matrix Spectra, Phys. Rev. Lett. **110**, 060602 (2013).

[82] V. Alba and F. Heidrich-Meisner, Entanglement spreading after a geometric quench in quantum spin chains, Phys. Rev. B **90**, 075144 (2014).

[83] M. Collura and G. Martelloni, Non-equilibrium transport in d-dimensional non-interacting Fermi gases, J. Stat. Mech. (2014) P08006.

[84] A. De Luca, G. Martelloni, and J. Viti, Stationary states in a free fermionic chain from the quench action method, Phys. Rev. A **91**, 021603(R) (2015).

[85] V. Eisler, F. Maislinger, and H. G. Evertz, Universal front propagation in the quantum Ising chain with domain-wall initial states, SciPost Phys. **1**, 014 (2016).

[86] J. Viti, J.-M. Stephan, J. Dubail, and M. Haque, Inhomogeneous quenches in a fermionic chain: Exact results, Europhys. Lett. **115**, 40011 (2016).

[87] M. Kormos, Inhomogeneous quenches in the transverse field Ising chain: Scaling and front dynamics, SciPost Phys. **3**, 020 (2017).

[88] G. Perfetto and A. Gambassi, Ballistic front dynamics after joining two semi-infinite quantum Ising chains, Phys. Rev. E **96**, 012138 (2017).

[89] L. Vidmar, D. Iyer, and M. Rigol, Emergent Eigenstate Solution to Quantum Dynamics Far from Equilibrium, Phys. Rev. X **7**, 021012 (2017).

[90] A. De Luca, J. Viti, L. Mazza, and D. Rossini, Energy transport in Heisenberg chains beyond the Luttinger liquid paradigm, Phys. Rev. B **90**, 161101 (2014).

[91] O. Castro-Alvaredo, Y. Chen, B. Doyon, and M. Hoogeveen, Thermodynamic Bethe ansatz for non-equilibrium steady states: Exact energy current and fluctuations in integrable QFT, J. Stat. Mech. (2014) P03011.

[92] A. Biella, A. De Luca, J. Viti, D. Rossini, L. Mazza, and R. Fazio, Energy transport between two integrable spin chains, Phys. Rev. B **93**, 205121 (2016).

[93] X. Zotos, F. Naef, and P. Prelovsek, Transport and conservation laws, Phys. Rev. B **55**, 11029 (1997).

[94] X. Zotos, Finite Temperature Drude Weight of the One-Dimensional Spin-1/2 Heisenberg Model, Phys. Rev. Lett. **82**, 1764 (1999).

[95] T. Prosen, Open XXZ Spin Chain: Nonequilibrium Steady State and a Strict Bound on Ballistic Transport, Phys. Rev. Lett. **106**, 217206 (2011).

[96] T. Prosen and E. Ilievski, Families of Quasilocal Conservation Laws and Quantum Spin Transport, Phys. Rev. Lett. **111**, 057203 (2013).

[97] E. Ilievski, M. Medenjak, and T. Prosen, Quasilocal Conserved Operators in the Isotropic Heisenberg Spin-1/2 Chain, Phys. Rev. Lett. **115**, 120601 (2015).

[98] F. Heidrich-Meisner, A. Honecker, D. C. Cabra, and W. Brenig, Zero-frequency transport properties of one-dimensional spin-$\frac{1}{2}$ systems, Phys. Rev. B **68**, 134436 (2003).

[99] D. Gobert, C. Kollath, U. Schollwöck, and G. Schütz, Real-time dynamics in spin-1/2 chains with adaptive time-dependent density matrix renormalization group, Phys. Rev. E **71**, 036102 (2005).

[100] S. Langer, F. Heidrich-Meisner, J. Gemmer, I. P. McCulloch, and U. Schollwöck, Real-time study of diffusive and ballistic transport in spin-1/2 chains using the adaptive time-dependent density matrix renormalization group method, Phys. Rev. B **79**, 214409 (2009).

[101] C. Karrasch, J. H. Bardarson, and J. E. Moore, Finite-Temperature Dynamical Density Matrix Renormalization Group and the Drude Weight of Spin-1/2 Chains, Phys. Rev. Lett. **108**, 227206 (2012).

[102] C. Karrasch, R. Ilan, and J. E. Moore, Nonequilibrium thermal transport and its relation to linear response, Phys. Rev. B **88**, 195129 (2013).

[103] O. A. Castro-Alvared, B. Doyon, and T. Yoshimura, Emergent Hydrodynamics in Integrable Systems Out of Equilibrium, Phys. Rev. X **6**, 041065 (2016).

[104] B. Bertini and M. Fagotti, Determination of the Nonequilibrium Steady State Emerging from a Defect, Phys. Rev. Lett. **117**, 130402 (2016).

[105] B. Doyon and T. Yoshimura, A note on generalized hydrodynamics: Inhomogeneous fields and other concepts, Scipost Phys. **2**, 014 (2017).

[106] A. De Luca, M. Collura, and J. De Nardis, Non-equilibrium spin transport in the XXZ chain: Steady spin currents and emergence of magnetic domains, Phys. Rev. B **96**, 020403 (2017).

[107] B. Doyon and H. Spohn, Dynamics of hard rods with initial domain wall state, J. Stat. Mech. (2017) P073210.

[108] B. Doyon, J. Dubail, R. Konik, and T. Yoshimura, Generalized Hydrodynamics and Density Waves in Interacting One-Dimensional Bose Gases, Phys. Rev. Lett. **119**, 195301 (2017).

[109] B. Doyon, H. Spohn, and T. Yoshimura, A geometric viewpoint on generalized hydrodynamics, Nucl. Phys. B **926**, 570 (2018).

[110] B. Doyon, T. Yoshimura, and J.-S. Caux, Soliton Gases and Generalized Hydrodynamics, Phys. Rev. Lett. **120**, 045301 (2018).

[111] V. B. Bulchandani, R. Vasseur, C. Karrasch, J. E. Moore, Bethe-Boltzmann Hydrodynamics and Spin Transport in the XXZ Chain, Phys. Rev. B **97**, 045407 (2018).

[112] V. B. Bulchandani, R. Vasseur, C. Karrasch, J. E. Moore, Solvable Hydrodynamics of Quantum Integrable Systems, Phys. Rev. Lett. **119**, 220604 (2018).

[113] E. Ilievski and J. De Nardis, On the Microscopic Origin of Ideal Conductivity, Phys. Rev. Lett. **119**, 020602 (2018).

[114] B. Doyon and H. Spohn, Drude Weight for the Lieb-Liniger Bose Gas, Scipost Phys. **3**, 039 (2017).

[115] V. Eisler and D. Bauernfeind, Front dynamics and entanglement in the XXZ chain with a gradient, Phys. Rev. B **96**, 174301 (2017).

[116] M. Fagotti, Higher-order generalized hydrodynamics in one dimension: The noninteracting test, Phys. Rev. B **96**, 220302(R) (2017).

[117] E. Ilievski and J. De Nardis, Ballistic transport in the one-dimensional Hubbard model: The hydrodynamic approach, Phys. Rev. B **96**, 081118(R) (2017).

[118] M. Collura, A. De Luca, J. Viti, Analytic solution of the Domain Wall non-equilibrium stationary state, Phys. Rev. B **97**, 081111(R) (2018).

[119] B. Doyon, Exact large-scale correlations in integrable systems out of equilibrium, SciPost Phys. **5**, 054 (2018).

[120] A. Bastianello, B. Doyon, G. Watts, T. Yoshimura, Generalized hydrodynamics of classical integrable field theory: The sinh-Gordon model, SciPost Phys. **4**, 045 (2018).

[121] J.-S. Caux, B. Doyon, J. Dubail, R. Konik, and T. Yoshimura, Hydrodynamics of the interacting Bose gas in the Quantum Newton Cradle setup, arXiv:1711.00873.

[122] E. Ilievski, J. De Nardis, M. Medenjak, and T. Prosen, Super-Diffusion in One-Dimensional Quantum Lattice Models, Phys. Rev. Lett. **121**, 230602 (2018).

[123] S. R. White and A. E. Feiguin, Real-Time Evolution Using the Density Matrix Renormalization Group, Phys. Rev. Lett. **93**, 076401 (2004).

[124] A. J. Daley, C. Kollath, U. Schollock, and G. Vidal, Time-dependent density-matrix renormalization-group using adaptive effective Hilbert spaces, J. Stat. Mech. (2004) P04005.

[125] U. Schollwöck, The density-matrix renormalization group, Rev. Mod. Phys. **77**, 259 (2005).

[126] U. Schollwöck, The density-matrix renormalization group in the age of matrix product states, Ann. Phys. **326**, 96 (2011).

[127] J. Hanus, Bound States in the Heisenberg Ferromagnet, Phys. Rev. Lett. **11**, 336 (1963).

[128] M. Wortis, Bound states of two spin waves in the Heisenberg ferromagnet, Phys. Rev. **132**, 85 (1963).

[129] H. C. Fogedby, The spectrum of continuous isotropic quantum Heisenberg chain: Quantum solitons as magnon bound states, J. Phys. C: Solid State Phys. **13**, L195 (1980).

[130] T. Schneider, Solitons and magnon bound states in ferromagnetic Heisenberg chains, Phys. Rev. B **24**, 5327 (1981).

[131] M. Ganahl, E. Rabel, F. H. L. Essler, H. G. Evertz, Observing Complex Bound States in the Spin-1/2 Heisenberg XXZ Chain, Phys. Rev. Lett. **108**, 077206 (2012).

[132] R. Vlijm, M. Ganahl, D. Fioretto, M. Brockmann, M. Haque, H. G. Evertz, and J.-S. Caux, Quasi-soliton scattering in quantum spin chains, Phys. Rev. B **92**, 214427 (2015).

[133] E. Haller, M. Gustavsson, M. J. Mark, J. G. Danzl, R. Hart, G. Pupillo, and H.-C. Nägerl, Relaization of an excited, strongly correlated quantum gas phase, Science **325**, 1224 (2009).

[134] T. Fukuhara, P. Schauss, M. Endres, S. Hild, M. Cheneau, I. Bloch, and C. Gross, Microscopic observation of magnon bound states and their dynamics, Nature (London) **502**, 76 (2013).

[135] M. Takahashi, *Thermodynamics of One-dimensional Solvable Models* (Cambridge University Press, Cambridge, 1999).

[136] E. Ilievski, E. Quinn, J. De Nardis, M. Brockmann, String-charge duality in integrable lattice models, J. Stat. Mech. (2016) 063101.

[137] J. R. Garrison and T. Grover, Does a Single Eigenstate Encode the Full Hamiltonian, Phys. Rev. X **8**, 021026 (2018).

[138] J.-S. Caux and F. H. L. Essler, Time Evolution of Local Observables After Quenching to An Integrable Model, Phys. Rev. Lett. **110**, 257203 (2013).

[139] J.-S. Caux, The Quench action, J. Stat. Mech. (2016) 064006.

[140] B. Wouters, J. De Nardis, M. Brockmann, D. Fioretto, M. Rigol, and J.-S. Caux, Quenching the Anisotropic Heisenberg Chain: Exact Solution and Generalized Gibbs Ensemble Predictions, Phys. Rev. Lett. **113**, 117202 (2014); M. Brockmann, B. Wouters, D. Fioretto, J. D. Nardis, R. Vlijm, and J.-S. Caux, Quench action approach for releasing the Néel state into the spin-1/2 XXZ chain, J. Stat. Mech. (2014) P12009.

[141] B. Pozsgay, M. Mestyán, M. A. Werner, M. Kormos, G. Zaránd, and G. Takács, Correlations after Quantum Quenches in the XXZ Spin Chain: Failure of the Generalized Gibbs

Ensemble, Phys. Rev. Lett. **113**, 117203 (2014); M. Mestyán, B. Pozsgay, G. Takács, and M. A. Werner, Quenching the XXZ spin chain: Quench action approach versus generalized Gibbs ensemble, J. Stat. Mech. (2015) P04001.

[142] V. Alba, and P. Calabrese, The quench action approach in finite integrable spin chains, J. Stat. Mech. (2016) 043105.

[143] A. Faribault, P. Calabrese, and J.-S. Caux, Quantum quenches from integrability: The fermionic pairing model, J. Stat. Mech. (2009) P03018; Bethe ansatz approach to quench dynamics in the Richardson model, J. Math. Phys. **50**, 095212 (2009).

[144] B. Pozsgay, Overlaps with arbitrary two-site states in the XXZ spin chain, J. Stat. Mech. (2018) 053103.

[145] V. Gritsev, T. Rostunov, and E. Demler, Exact methods in the analysis of the non-equilibrium dynamics of integrable models: Application to the study of correlation functions for non-equilibrium 1D Bose gas, J. Stat. Mech. (2010) P05012.

[146] B. Pozsgay, Overlaps between eigenstates of the XXZ spin-1/2 chain and a class of simple product states, J. Stat. Mech. (2014) P06011.

[147] J. De Nardis, B. Wouters, M. Brockmann, and J.-S. Caux, Solution for an interaction quench in the Lieb-Liniger Bose gas, Phys. Rev. A **89**, 033601 (2014).

[148] M. Brockmann, J. D. Nardis, B. Wouters, and J.-S. Caux, A Gaudin-like determinant for overlaps of Néel and XXZ Bethe states, J. Phys. A: Math. Theor. **47**, 145003 (2014); M. Brockmann, Overlaps of q-raised Néel states with XXZ Bethe states and their relation to the Lieb-Liniger Bose gas, J. Stat. Mech. (2014) P05006; M. Brockmann, J. De Nardis, B. Wouters, and J.-S. Caux, Néel-XXZ state overlaps: Odd particle numbers and Lieb-Liniger scaling limit, J. Phys. A: Math. Theor. **47**, 345003 (2014).

[149] P. Le Doussal and P. Calabrese, The KPZ equation with flat initial condition and the directed polymer with one free end, J. Stat. Mech. (2012) P06001; P. Calabrese and P. Le Doussal, Interaction quench in a Lieb-Liniger model and the KPZ equation with flat initial conditions, *ibid.* (2014) P05004.

[150] L. Piroli and P. Calabrese, Recursive formulas for the overlaps between Bethe states and product states in XXZ Heisenberg chains, J. Phys. A: Math. Theor. **47**, 385003 (2014).

[151] M. de Leeuw, C. Kristjansen, and K. Zarembo, One-point functions in defect CFT and integrability, J. High Energy Phys. 08 (2015) 098; I. Buhl-Mortensen, M. de Leeuw, C. Kristjansen, and K. Zarembo, One-point Functions in AdS/dCFT from Matrix Product States, *ibid.* 02 (2016) 052; O. Foda and K. Zarembo, Overlaps of partial Néel states and Bethe states, J. Stat. Mech. (2016) 023107.

[152] M. de Leeuw, C. Kristjansen, and S. Mori, AdS/dCFT one-point functions of the SU(3) sector, Phys. Lett. B **763**, 197 (2016).

[153] D. X. Horváth, S. Sotiriadis, and G. Takács, Initial states in integrable quantum field theory quenches from an integral equation hierarchy, Nucl. Phys. B **902**, 508 (2016); D. X. Horváth and G. Takács, Overlaps after quantum quenches in the sine-Gordon model, Phys. Lett. B **771**, 539 (2017).

[154] P. P. Mazza, J.-M. Stéphan, E. Canovi, V. Alba, M. Brockmann, and M. Haque, Overlap distributions for quantum quenches in the anisotropic Heisenberg chain, J. Stat. Mech. (2016) 013104.

[155] B. Pozsgay and V. Eisler, Real-time dynamics in a strongly interacting bosonic hopping model: Global quenches and mapping to the XX chain, J. Stat. Mech. (2016) 053107.

[156] B. Bertini, D. Schuricht, and F. H. L. Essler, Quantum quench in the sine-Gordon model, J. Stat. Mech. (2014) P10035.

[157] B. Bertini, L. Piroli, and P. Calabrese, Quantum quenches in the sinh-Gordon model: Steady state and one-point correlation functions, J. Stat. Mech. (2016) 063102.

[158] B. Bertini, E. Tartaglia, and P. Calabrese, Quantum Quench in the Infinitely Repulsive Hubbard Model: The Stationary State, J. Stat. Mech. (2017) 103107.

[159] L. Piroli, P. Calabrese, and F. H. L. Essler, Multiparticle Bound-State Formation following a Quantum Quench to the One-Dimensional Bose Gas with Attractive Interactions, Phys. Rev. Lett. **116**, 070408 (2016); Quantum quenches to the attractive one-dimensional Bose gas: Exact results, SciPost Phys. **1**, 001 (2016).

[160] L. Piroli, B. Pozsgay, and E. Vernier, What is an integrable quench? Nucl. Phys. B **925**, 362 (2017).

[161] G. Delfino, Quantum quenches with integrable pre-quench dynamics, J. Phys. A: Math. Theor. **47**, 402001 (2014).

[162] L. Piroli, E. Vernier, and P. Calabrese, Exact steady states for quantum quenches in integrable Heisenberg spin chains, Phys. Rev. B **94**, 054313 (2016).

[163] L. Bonnes, F. H. L. Essler, and A. M. Läuchli, "Light-cone" Dynamics After Quantum Quenches in Spin Chains, Phys. Rev. Lett. **113**, 187203 (2014).

[164] For the implementation we used the ITENSOR library (http://itensor.org/).

[165] P. Ruggiero, V. Alba, and P. Calabrese, Entanglement negativity in random spin chains, Phys. Rev. B **94**, 035152 (2016).

[166] V. Alba, B. Bertini, and M. Fagotti (unpublished).